

Diurnal proteome profile of the mouse cerebral cortex

Conditional deletion of the Bmal1 circadian clock gene elevates astrocyte protein levels and cell abundance in the neocortex and hippocampus

Bering, Tenna; Gadgaard, Camilla; Vorum, Henrik; Honoré, Bent; Rath, Martin Fredensborg

Published in:
Glia

DOI (link to publication from Publisher):
[10.1002/glia.24443](https://doi.org/10.1002/glia.24443)

Creative Commons License
CC BY 4.0

Publication date:
2023

Document Version
Publisher's PDF, also known as Version of record

[Link to publication from Aalborg University](#)

Citation for published version (APA):

Bering, T., Gadgaard, C., Vorum, H., Honoré, B., & Rath, M. F. (2023). Diurnal proteome profile of the mouse cerebral cortex: Conditional deletion of the Bmal1 circadian clock gene elevates astrocyte protein levels and cell abundance in the neocortex and hippocampus. *Glia*, 71(11), 2623-2641. <https://doi.org/10.1002/glia.24443>

General rights

Copyright and moral rights for the publications made accessible in the public portal are retained by the authors and/or other copyright owners and it is a condition of accessing publications that users recognise and abide by the legal requirements associated with these rights.






- Users may download and print one copy of any publication from the public portal for the purpose of private study or research.
- You may not further distribute the material or use it for any profit-making activity or commercial gain
- You may freely distribute the URL identifying the publication in the public portal -

Take down policy

If you believe that this document breaches copyright please contact us at vbn@aub.aau.dk providing details, and we will remove access to the work immediately and investigate your claim.

RESEARCH ARTICLE

Diurnal proteome profile of the mouse cerebral cortex: Conditional deletion of the *Bmal1* circadian clock gene elevates astrocyte protein levels and cell abundance in the neocortex and hippocampus

Tenna Bering¹  | Camilla Gadgaard¹  | Henrik Vorum^{2,3}  | Bent Honoré^{3,4}  | Martin Fredensborg Rath¹ 

¹Department of Neuroscience, Faculty of Health and Medical Sciences, University of Copenhagen, Copenhagen, Denmark

²Department of Ophthalmology, Aalborg University Hospital, Aalborg, Denmark

³Department of Clinical Medicine, Faculty of Medicine, Aalborg University, Aalborg, Denmark

⁴Department of Biomedicine, Faculty of Health, Aarhus University, Aarhus, Denmark

Correspondence

Martin Fredensborg Rath, Department of Neuroscience, University of Copenhagen, Panum Institute 24.6.06, Blegdamsvej 3B, Copenhagen DK-2200, Denmark.
 Email: mrath@sund.ku.dk

Funding information

A.P. Møller og Hustru Chastine McKinney Møllers Fond til Almene Formaal; Danmarks Frie Forskningsfond, Grant/Award Number: 1030-00045B; Læge Sofus Carl Emil Friis og hustru Olga Doris Friis' Legat; Lundbeckfonden, Grant/Award Numbers: R108-A10301, R344-2020-261; Novo Nordisk Fonden, Grant/Award Number: NNF21OC007021

Abstract

Circadian oscillators, defined by cellular 24 h clock gene rhythms, are found throughout the brain. Cerebral cortex-specific conditional knockout of the clock gene *Bmal1* (*Bmal1* CKO) leads to depressive-like behavior, but the molecular link from clock gene to altered behavior is unknown. Further, diurnal proteomic data on the cerebral cortex are currently unavailable. With the aim of determining the diurnal proteome profile and downstream targets of the cortical circadian clock, we here performed a proteomic analysis of the mouse cerebral cortex. Proteomics identified approximately 2700 proteins in both the neocortex and the hippocampus. In the neocortex, 15 proteins were differentially expressed (>2-fold) between day and night, mainly mitochondrial and neuronal plasticity proteins. Only three hippocampal proteins were differentially expressed, suggesting that daily protein oscillations are more prominent in the neocortex. The number of differentially expressed proteins was reduced in the *Bmal1* CKO, suggesting that daily rhythms in the cerebral cortex are primarily driven by local clocks. The proteome of the *Bmal1* CKO cerebral cortex was dominated by upregulated proteins expressed in astrocytes, including GFAP (4-fold) and FABP7 (>20-fold), in both the neocortex and hippocampus. These findings were confirmed at the transcript level. Cellular analyses of astrocyte components revealed an increased number of GFAP-positive cells in the *Bmal1* CKO cerebral cortex. Further, BMAL1 was found to be expressed in both GFAP- and FABP7-positive astrocytes of control animals. Our data show that *Bmal1* is required for proper cellular composition of the cerebral cortex, suggesting that increased cortical astrocyte activity may induce behavioral changes.

Abbreviations: *Bmal1*, basic helix-loop-helix ARNT like 1 (previously known as *Arntl*); CKO, conditional knockout; CT, circadian time; DD, dark:dark schedule (darkness); LC-MS/MS, liquid chromatography-tandem mass spectrometry; LFQ, label-free quantification; qRT-PCR, quantitative reverse-transcription real-time PCR; LD, 12 h light:12 h dark schedule; SCN, suprachiasmatic nucleus; ZT, Zeitgeber time.

This is an open access article under the terms of the [Creative Commons Attribution](https://creativecommons.org/licenses/by/4.0/) License, which permits use, distribution and reproduction in any medium, provided the original work is properly cited.

© 2023 The Authors. GLIA published by Wiley Periodicals LLC.

KEYWORDS

astrocyte, *Bmal1*, clock gene, conditional knockout mouse, glial marker, hippocampus, neocortex, proteomics

1 | INTRODUCTION

Circadian rhythms, that is, 24 h endogenous biological rhythms, are maintained by a molecular circadian clock that enables living organisms to efficiently synchronize physiological functions to the light regime (Takahashi, 2017). Anatomically, the master clock of mammals resides in neurons of the suprachiasmatic nucleus (SCN), but the molecular clock, as defined by oscillating clock gene expression, is a feature of most if not all cell types (Guilting & Piggins, 2007). In this regard, oscillating circadian clock gene expression has been reported in all major regions of the brain, including neurons of the neocortex (Rath et al., 2013; Rath et al., 2014) and the hippocampus (Honma et al., 1998; Jilg et al., 2010). While rhythmic clock gene expression in the cerebral cortex seems to depend on a circadian input from the SCN (Rath et al., 2013), the functional role of these extrahypothalamic molecular brain oscillators is far less understood. Evidence from studies in humans shows a clear correlation between major depressive disorder and altered clock gene expression in both neocortical and hippocampal areas of the cerebral cortex (Li et al., 2013), suggesting that local changes in clock gene accompanies development of depression; however, the link between brain disorders and circadian dysfunction is largely correlational (Logan & McClung, 2019).

To clarify a possible causal link from disrupted clock gene expression in extrahypothalamic circadian oscillators to altered behavior, we previously generated a mouse strain in which the canonical clock gene *Bmal1* (basic helix–loop–helix ARNT like 1, previously known as *Arntl*) was specifically deleted in the cerebral cortex by use of Cre-LoxP technology (Bering et al., 2018). In this *Bmal1* conditional knockout (CKO) model, the Cre-recombinase is driven by the promoter of *Emx1* (Guo et al., 2000), which allows us to specifically disrupt the circadian clock in the cerebral cortex, including the neocortex and the hippocampus, while leaving the master clock of the SCN intact (Bering et al., 2018). The *Bmal1* CKO showed only minor changes in circadian locomotor rhythmicity, whereas a phenotype with depressive-like behavior and reduced monoamine signaling was evident, suggesting that a circadian malfunction of the clock of the cerebral cortex is a causal component in development of depressive disorder (Bering et al., 2018; Li et al., 2013); however, the molecular connection from the circadian clock of the cerebral cortex to affective behavior still represents a missing link in our understanding of the circadian system of the brain.

Circadian clock gene expression profiles in the cerebral cortex, that is, both the neocortex and the hippocampus, are well documented; also, the daily profiles of gene expression in the mouse neocortex and the hippocampus have been analyzed by microarray and RNA sequencing (Hor et al., 2019; Lananna et al., 2018; Renaud et al., 2015). However, large-scale screening efforts of protein contents of the mouse cerebral cortex so far did not include temporal profiles (Sharma et al., 2015); therefore, general day-night changes in

the murine neocortical and hippocampal proteome, which would represent a first-step towards identifying clock-controlled proteins, still represent a gap in our knowledge on circadian biology of the cerebral cortex.

With the purpose to determine daily changes in protein expression in the cerebral cortex and to identify downstream molecular targets of the *Bmal1*-dependent circadian clock, we here performed proteomic analyses of the neocortex and the hippocampus of normal mice and a *Bmal1* CKO model, respectively. The results of these efforts, which would represent an initial link between a disrupted local clock and altered behavior, are presented below.

2 | MATERIALS AND METHODS

2.1 | Animals

Bmal1 conditional knockout mice (*Bmal1* CKO; *Emx1*-Cre⁺/*Bmal1*-flox^{+/+}) and control mice (*Emx1*-Cre⁻/*Bmal1*-flox^{+/+}) were generated by crossing of a *Bmal1*-flox carrying strain (B6.129S4 (Cg)-*Arntl*^{tm1Weit}/J; stock number 7668; *Bmal1* previously known as *Arntl*) (Storch et al., 2007) and a homozygote *Emx1*-Cre carrying strain (B6.129S2-*Emx1*^{tm1(cre)Krl}/J; stock number 5628) (Guo et al., 2000) obtained from Jackson Laboratories (Charles River, Sulzfeld, Germany). The *Emx1*-Cre carrying strain has been previously characterized and exhibits a high (>90%) LoxP-specific recombination efficiency (Guo et al., 2000). The mice were housed under controlled light conditions in a 12 h light:12 h dark (LD) schedule with food and water ad libitum. Breeding and genotyping were performed as previously described (Bering et al., 2018). BMAL1 protein was absent in the neocortex and hippocampus of the *Bmal1* CKO, but still detectable in the SCN (Figure S1). Disrupted clock gene rhythms in the cerebral cortex and behavioral characterization have been previously reported (Bering et al., 2018).

For proteomic analyses, a total of 26 mice were sacrificed by decapitation; the neocortex and the hippocampus were dissected and immediately frozen on dry ice; animals included *Bmal1* CKO mice sacrificed at Zeitgeber time (ZT) 6 (3 male, 5 female, 24–76 weeks of age), *Bmal1* CKO mice sacrificed at ZT18 (3 male, 4 female, 20–63 weeks of age) and control mice sacrificed at ZT6 (3 male, 2 female, 18–65 weeks of age) and ZT18 (2 male, 4 female, 18–63 weeks of age), respectively. For quantitative reverse-transcription real-time PCR (qRT-PCR), a total of 48 animals were kept in darkness (DD) for 2 days and sacrificed by decapitation in three-hour intervals throughout the presumptive day and night; the neocortex and the hippocampus were dissected and immediately frozen on dry ice; animals included 24 *Bmal1* CKO mice (11 male, 13 female, 13–25 weeks of age) and 24 control mice (15 male, 9 female, 13–23 weeks of age). For radiochemical in situ hybridization, a total

of 38 mice were sacrificed by decapitation in four-hour intervals; the brains were removed and frozen in crushed dry ice; animals included 20 *Bmal1* CKO mice (10 male, 10 female, 14–17 weeks of age) and 18 control mice (12 male, 6 female, 13–19 weeks of age). Samples from mice included in the qRT-PCR and in situ hybridization analyses presented here have also been used in a previous publication (Bering et al., 2018). For immunohistochemistry, animals were anesthetized with tribromoethanol (400 mg/kg) at ZT5 and sacrificed by transcardial perfusion with PBS (with heparin) followed by 4% paraformaldehyde in 0.1 M phosphate buffer (pH 7). The brains were removed, postfixed for 48 h in the same fixative, cryoprotected in 25% sucrose in PBS for 48 h and finally frozen in crushed dry ice; animals included four *Bmal1* CKO mice (3 male, 1 female, 10–13 weeks of age) and four control mice (1 male, 3 female, 9–22 weeks of age).

All animal experiments were performed in accordance with the guidelines of EU Directive 2010/63/EU and the specific experiments in this study were approved by the Danish Council for Animal Experiments (authorization number 2017-15-0201-01190) and the Faculty of Health and Medical Sciences, University of Copenhagen (authorization number P21-146).

2.2 | Proteomics

The experimental approach is summarized in Figure 1. Samples were prepared for analysis with the suspension trapping method (Zougman et al., 2014) using S-Trap spin columns (Protifi). Label-free quantification (LFQ) liquid chromatography–tandem mass spectrometry (LC–MS/MS) was performed with the universal methods settings,

essentially as previously described (Ludvigsen et al., 2020). In short, 1 µg of each sample was run in triplicate on a Dionex Ultimate™ 3000RSLC system connected to an Orbitrap Fusion Tribrid mass spectrometer with an EasySpray™ ion source (Thermo Scientific). MaxQuant software version 1.6.6.0 (Tyanova, Temu, & Cox, 2016) was used to perform a search of the raw data files against the reviewed UniProt *Mus musculus* database (downloaded on September 2, 2019). The ProteinGroup data file was subsequently analyzed in Perseus software version 1.6.6.0 (Tyanova, Temu, Sinitcyn, et al., 2016). Identification of a protein required at least two unique peptides; quantitative values were log₂-transformed. Proteins were identified in at least 70% of the samples in each group compared.

Pathway analyses were performed using the online PANTHER Overrepresentation Test (pantherdb.org) in annotation version GO Ontology database DOI: <http://doi.org/10.5281/zenodo.6799722> released July 1, 2022. Differentially expressed proteins were tested for overrepresentation of the annotation data sets “GO biological process complete” and “GO molecular function complete.” These proteins were tested against two separate reference lists, the full *Mus musculus* gene database provided in PANTHER, but also the list of proteins detected in the mass spectrometry. Analyses were set to use Fisher's Exact test type corrected for calculated false discovery rate.

2.3 | Quantitative RT-PCR

qRT-PCR was performed as previously described (Bering et al., 2017; Bering et al., 2018; Rath et al., 2014). Briefly, RNA was isolated from neocortices and hippocampi by use of TRIzol reagent, DNase treated,

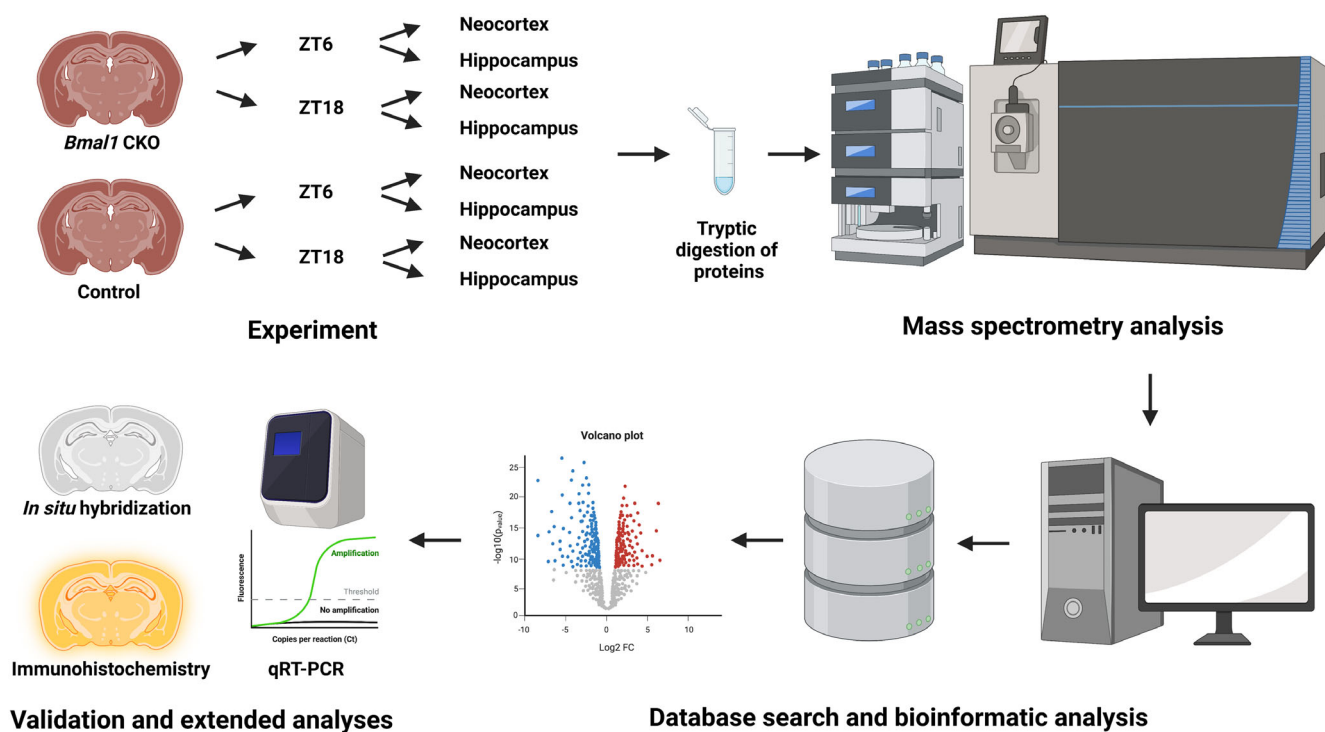


FIGURE 1 Flowchart of experimental approach. Figure was created by use of BioRender.

and 500 ng was reverse transcribed by use of Superscript III (Invitrogen). PCR reactions were run in a Lightcycler 96 (Roche) with 10 μ L reactions containing 0.5 μ M primers (Table 1), FastStart Essential DNA Green Master (Roche) and 0.2 μ L cDNA. Transcript copy numbers were determined by use of internal 10-fold dilutions of pUC57 plasmids containing the sequence to be amplified (GenScript) and normalized against the geometric mean of *Actb* and *Gapdh* copy numbers.

2.4 | Radiochemical in situ hybridization

Radiochemical in situ hybridization was performed as previously described (Rath & Moller, 2022). In brief, DNA oligo probes targeting two regions of the transcript of interest (Table 2) were labeled with [35 S]dATP (Perkin Elmer) by use of terminal transferase (Sigma). Cryostat sections (12 μ m) of unfixed brains mounted on slides were fixed in formaldehyde, acetylated, dehydrated in a graded series of ethanol, and delipidated in chloroform. Sections were incubated with the labeled probe overnight at 37°C, washed in SSC, and exposed to an x-ray film for 3 weeks. Autoradiographs were digitized and optical densities of the neocortex and the dorsal hippocampus were measured in Scion Image and converted to dpm/mg tissue by use of simultaneously exposed 14 C standards (Amersham).

2.5 | Immunohistochemistry

Immunohistochemistry was performed on free-floating cryostat sections (40 μ m) as previously described (Rath et al., 2014). In brief, sections were blocked in serum and incubated in different combinations of primary antibodies against FABP7, GFAP, and BMAL1 overnight (Table 3). Sections were subsequently incubated in fluorophore-conjugated secondary antibodies (Table 3) or, in case of FABP7, in a biotinylated secondary antibody, followed by ABC

Vectastain (Vector Laboratories), tyramide signal amplification (TSA) (Perkin Elmer) and a streptavidin-fluorophore conjugate (Table 3). All sections were finally stained in DAPI before mounting on slides. Sections from at least three animals of each genotype (*Bmal1* CKO and controls) were run and analyzed in parallel. Sections were photographed in an LSM980 inverted laser scanning confocal microscope (Zeiss). Adjustments of light and contrast and image overlays were done using ZEN2.3 pro software (Zeiss); images from all animals were processed using identical settings.

The specificity of the antibodies against GFAP and BMAL1 has been previously tested (Rath et al., 2014). However, to test the specificity of the antibody against FABP7, the diluted antibody was preincubated with the immunogen mouse BLBP peptide (Abcam, catalogue number ab32422) at a concentration of 100 μ g/mL for 6 days prior to incubation of the sections. Preabsorption completely abolished the immunohistochemical signal in both the neocortex and hippocampus (Figure S2).

To determine the number of GFAP-positive cells, the dentate gyrus or layer two of the neocortex located above the dentate gyrus were identified in DAPI staining, the filter set of the microscope was switched without changing the position of the slide, and the immunohistochemical signal was photographed. Three brain sections from each mouse were photographed (total of six photographs per mouse). Each photograph corresponded to a tissue volume of 561 μ m (horizontal) \times 361 μ m (vertical) \times 40 μ m (section thickness). GFAP-immunopositive cell bodies in the images were counted blinded. In the same photographs, GFAP-signal intensity was measured in individual cell bodies by use of Scion Image Beta version 4.0.02 (Scion), also blinded.

2.6 | Statistics

Quantitative proteome data (LFQ data) were analyzed in Perseus software version 1.6.6.0 by Student's *t*-test. An uncorrected two-tailed *p*-value of .01 was considered to represent statistical significance.

TABLE 1 qRT-PCR primer sequences.

Transcript	GenBank accession number	Position	Forward primer sequence (5'–3')	Reverse primer sequence (5'–3')
<i>Fabp7</i>	NM_021272.3	414–543	AAGGATGGCAAGATGGTCGT	TAGCTGGCTAACTCTGGGACT
<i>Gfap</i>	NM_001131020.1	645–874	GAATCGCTGGAGGAGGAGAT	GCGTCTGTGAGGTCTGCAA
<i>Dbi</i>	NM_001037999.2	193–336	GCCTCAAGACTCAGCCAAC	TCAGCTTGTCCACGAGTCC
<i>Gng4</i>	NM_010317.3	523–648	AGATGGAAGCCTGCATGGAC	GGAAGGGGTTTCTGAGGCA
<i>Actb</i>	NM_007393.3	54–257	CGGTCCACACCCGCCACCA	TCTGGGCTCTGCACCCACAT
<i>Gapdh</i>	NM_008084.2	20–122	TGTGCAGTGCCAGCCTCGTC	GCCACTGCAAATGGCAGCCC

TABLE 2 In situ hybridization probe sequences.

Transcript	GenBank accession number	Position	Probe sequence (5'–3')
<i>Gfap</i>	NM_001131020.1	699–664	GAACCTCCTCCTCATAGATCTTCCTTAAGAACTGGA
		216–182	CAGGGAGTGGAGGAGTCATTCGAGACAAGGAGAAG
<i>Fabp7</i>	NM_021272.3	333–298	ACTTACAGTTTCTGTCTATGCTGGTTTCTTCAA
		429–394	CCATCTTGCCATCCTTAATTTCTCTGGTACAATTG

TABLE 3 Antibodies used for immunohistochemistry.

Protein target	Primary antibody			Secondary antibody			Conjugate after TSA		
	Name	Vendor, catalogue number	Dilution	Name	Vendor, catalogue number	Dilution	Name	Vendor, catalogue number	Dilution
FABP7	Rabbit anti-BLBP	Abcam, ab32423	1/1000	Donkey anti-rabbit IgG, biotin	Jackson, 711-065-152	1/500	Alexa Fluor 568, streptavidin	Invitrogen, S11226	1/400
GFAP	Mouse anti-GFAP, clone GA5	Millipore, MAB360	1/400	Alexa Fluor 488 donkey anti-mouse IgG	Invitrogen, A21202	1/400	TSA not used		
BMAL1	Goat anti-BMAL1 (N-20)	Santa Cruz, sc-8550	1/200	Alexa Fluor 647 donkey anti-goat IgG	Invitrogen, A21447	1/400			

Quantitative data obtained by qRT-PCR and radiochemical in situ hybridization were analyzed in Prism 9.0.4 (GraphPad) by two-way ANOVA followed by Bonferroni-multiple comparison's post hoc test or one-way ANOVA; data are presented as individual measurements with mean. Cell counts and signal intensities based on immunohistochemical reactions were analyzed in Prism 9.0.4 by use of Mann-Whitney U-test and Student's *t*-test, respectively. Data are presented as individual values with mean and standard error of mean. Total number of animals (with gender and age) for each experiment are given in the *Animals* sections above; *n*-values are given in figure legends. A two-tailed *p*-value of .05 was considered to represent statistical significance.

3 | RESULTS

3.1 | Mitochondrial, cytoskeletal, and neuronal plasticity proteins are differentially expressed between day and night in the mouse cerebral cortex, but rhythmic expression mainly depends on local expression of *Bmal1*

The proteome of the mouse cerebral cortex has been previously reported (Sharma et al., 2015), but the daily profile is unknown. As a first step towards characterizing proteins potentially regulated by the local circadian clock of the cerebral cortex, we therefore identified the proteome of the neocortex and hippocampus from both control and *Bmal1* CKO mice at ZT6 and ZT18 (Tables S1–S4). A total of 2778 proteins were detected in the neocortex, whereas a

total of 2695 proteins were detected in the hippocampus: among these, 2455 proteins were detected in both tissues with 309 detected exclusively in the neocortex and 227 detected exclusively in the hippocampus. Notably, clock gene products, including BMAL1, were not detected.

To identify proteins differentially expressed between day and night, proteomic data from samples collected at ZT18 and ZT6 were compared. Cut-off was set at >2-fold changes combined with *p*-values <.01 (Figures 2 and 3a, Table 4). Using these criteria, 15 proteins (COX6A1, COX6C, UQCRB, UQCRQ, NDUFB1, LZTFL1, LPHN3, SNCB, GNG12, GNG4, GLTP, DBI, TUBB6, ABRACL, and ARPC3) were identified as being differentially expressed in the neocortex of the control mouse with 13 proteins upregulated at ZT6 and two upregulated at ZT18 (Figure 2a). Among these, five proteins of the mitochondrial respiratory chain were upregulated at daytime (COX6A1, COX6C, UQCRB, UQCRQ, and NDUFB1). Other daytime proteins included proteins involved in neural plasticity (LZTFL1, LPHN3, and SNCB), G-proteins (GNG12 and GNG4), proteins involved in lipid transport and metabolism (GLTP and DBI), whereas the two proteins upregulated in the nighttime samples and one upregulated during daytime were cytoskeletal (TUBB6, ABRACL, and ARPC3) (Table 4). Pathway analysis revealed an overrepresentation of proteins related to aerobic electron transport chain and mitochondrial ATP synthesis coupled electron transport in the group of 15 proteins differentially expressed between night and day samples in the neocortex of the control mouse (Figure S3). In the hippocampus, only three proteins (PCSK1N, TMSB4X, and PPP1R1A) were differentially expressed between day and night (Figure 2b), all upregulated

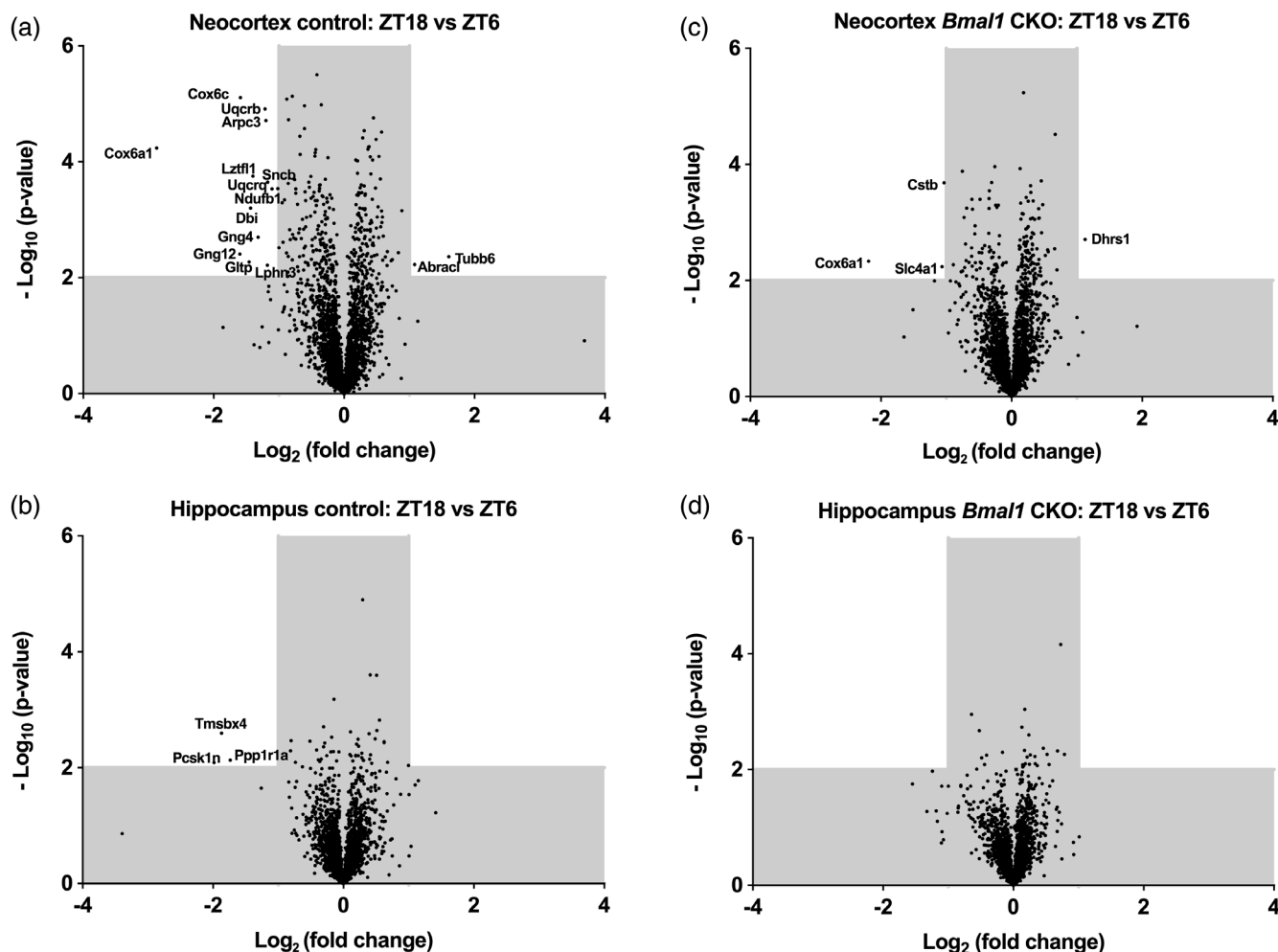


FIGURE 2 Day-night changes in the proteome of the mouse cerebral cortex. Volcano plots of proteomic analyses of differential expression of proteins between night (ZT18) and day (ZT6) in the neocortex of the control mouse (a), the hippocampus of the control mouse (b), the neocortex of the *Bmal1* CKO mouse (c), and the hippocampus of the *Bmal1* CKO mouse (d). For each identified protein, the negative \log_{10} of the p -value (Student's t -test) is plotted against the \log_2 of the detected fold change calculated as the mean value at ZT18 divided by the mean value at ZT6. Proteins with $p < .01$ and fold change > 2.0 were regarded as being differentially expressed and were included in further analyses (Table 4); shaded areas indicate these cut-off values with proteins that were not included in further analyses. $n = 5$ –8 in each experimental group.

during daytime, with diverse functions such as regulation of neuroendocrine pathways (PCSK1N), stem cell differentiation (TMSBX4) and glycogen metabolism (PPP1R1A) (Table 4).

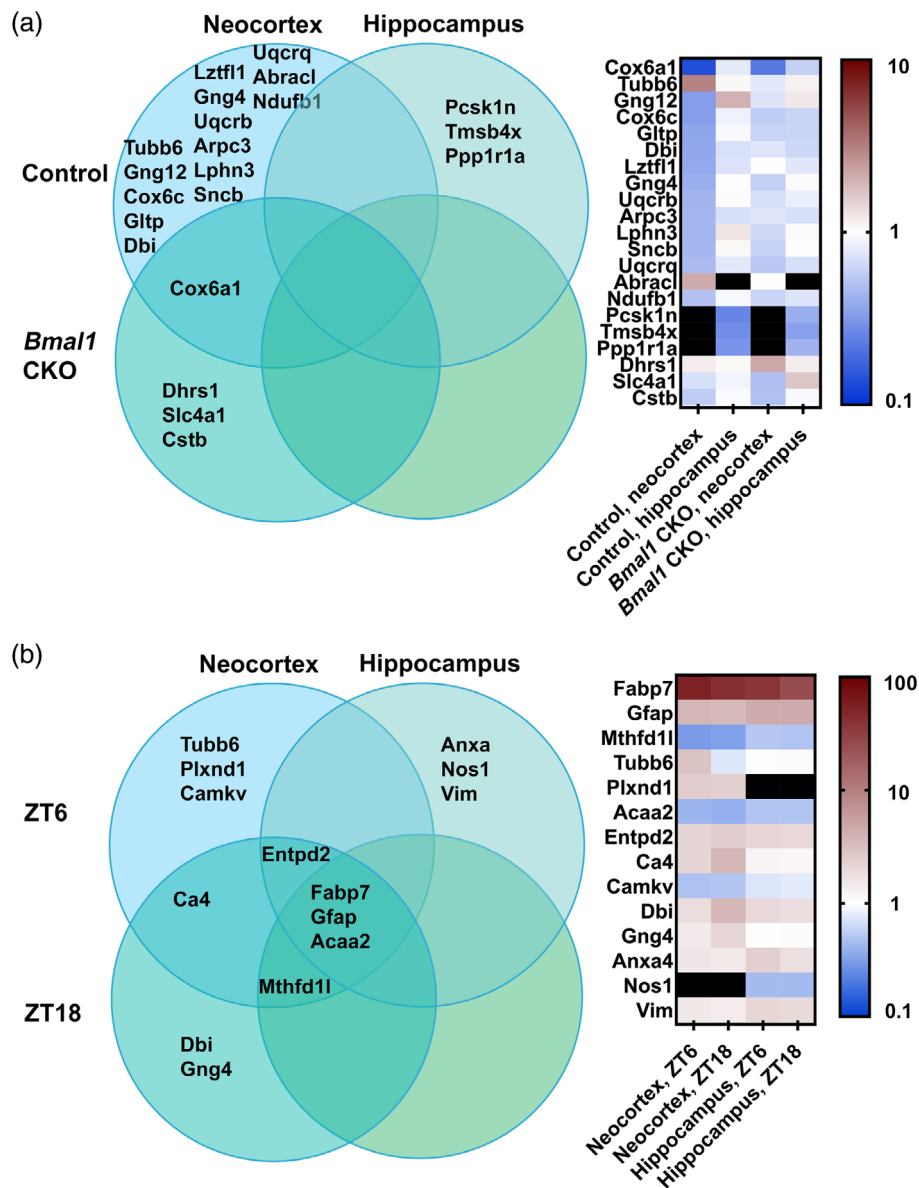
In the neocortex of the *Bmal1* CKO mouse, four proteins (COX6A1, DHRS1, SLC4A1, and CSTB) were found to be differentially expressed (Figure 2c), including daytime upregulation of the mitochondrial respiratory chain protein that exhibited the most prominent change in the neocortex of the control mouse (COX6A1). Other rhythmic proteins in the neocortex of the *Bmal1* CKO mouse had diverse functions (Table 4), such as steroid metabolism (DHRS1), ion transport (SLC4A1) and proteinase inhibition (CSTB). Using the criteria detailed above, differential protein expression between day and night was not detected in the hippocampus of the *Bmal1* CKO mouse (Figure 2d). In summary, this part of our proteomic analysis suggests that the day-night differences in the proteome of the neocortex are more

abundant than those of the hippocampus and that rhythmic protein expression to some extent requires an intact local circadian clock in the brain region itself.

3.2 | Proteins known to be expressed in astrocytes are upregulated in both the neocortex and hippocampus of the *Bmal1* CKO mouse

To identify proteins differentially expressed between genotypes, proteomic data from samples collected from both the neocortex and hippocampus at ZT18 and ZT6 were compared between the *Bmal1* CKO mouse and the control (Tables S5–S8). Again, cut-off was set at > 2 -fold changes combined with p -values $< .01$ (Figures 3b and 4, Table 5). Fourteen proteins (FABP7, GFAP, MTHFD1L, TUBB6,

FIGURE 3 Summary of proteomic data. (a) Day-night changes in the proteome of the neocortex and hippocampus in the control and *Bmal1* CKO mouse, respectively. Data from Figure 2 and Table 4 displayed as a Venn diagram and a heatmap. Rhythmic proteins are mainly detected in the neocortex of the control mouse. (b) *Bmal1*-dependent changes in the proteome of the neocortex and hippocampus at ZT6 and ZT18, respectively. Data from Figure 4 and Table 5 displayed as a Venn diagram and a heatmap. FABP7 and GFAP are highly upregulated in the *Bmal1* CKO at both timepoints in both tissues. Black cells in the heat maps indicate that the protein was not detectable.



PLXND1, ACAA2, ENTPD2, CA4, CAMKV, DBI, GNG4, ANXA4, NOS1, and VIM) were found to be differentially expressed between genotypes in at least one brain region at one time point. In the neocortex, 12 proteins (FABP7, GFAP, MTHFD1L, TUBB6, PLXND1, ACAA2, ENTPD2, CA4, CAMKV, DBI, and GNG4) were identified, with six of these being differentially expressed at both time points (FABP7, GFAP, MTHFD1L, ACAA2, ENTPD2, and CA4). In the hippocampus, eight proteins (FABP7, GFAP, MTHFD1L, ACAA2, ENTPD2, ANXA4, NOS1, and VIM) were identified, with three proteins being differentially expressed at both time points (FABP7, GFAP, and ACAA2), all of which were also differentially expressed at both time points in the neocortex.

In both the neocortex and the hippocampus and at both time points examined, FABP7, a protein involved in radial glial cell function, and GFAP, a cytoskeletal protein in astrocytes, were found to be highly upregulated in the *Bmal1* CKO. GFAP is a well-established astrocyte marker (Middeldorp & Hol, 2011), while FABP7 in addition to

oligodendrocyte precursor cells is also expressed in astrocytes of the adult rodent brain (Foerster et al., 2020; Schmid et al., 2006; Sharifi et al., 2011; Sharifi et al., 2013), thus suggesting that astrocytes may be heavily affected by the knockout of the circadian clock. On the other hand, mitochondrial proteins (MTHFD1L and ACAA2) were generally downregulated in the neocortex and hippocampus of the *Bmal1* CKO. In addition, the enzyme ENTPD2, which is involved in extracellular signaling during neurogenesis (Gampe et al., 2015), was upregulated in both the neocortex and the hippocampus. Other proteins were affected by *Bmal1* knockout in one brain region only (Figure 4, Table 5).

In the neocortex, the cytoskeletal protein TUBB6, which was identified as being rhythmic in the control mouse with upregulation during nighttime (Figure 2a, Table 4), was found to be upregulated in the day-time samples of the *Bmal1* CKO neocortex (Figure 4a, Table 5) reflecting the loss of daily rhythm in the *Bmal1* CKO cerebral cortex. Similarly, GNG4, a G-protein, and DBI, which is involved in lipid metabolism, both exhibited differential diurnal expression in the control mouse with

TABLE 4 Differential expression of proteins between day (ZT6) and night (ZT18) in neocortical and hippocampal samples collected from *Bmal1* CKO and control mice, respectively.

Protein name	Gene symbol	Protein ID	Night-day ratio				Function (uniprot.org)
			Control		Bmal1 CKO		
			Neocortex	Hippocampus	Neocortex	Hippocampus	
Cytochrome c oxidase subunit 6A1, mitochondrial	Cox6a1	P43024	7.34 ⁻¹		4.56 ⁻¹		Mitochondrial respiratory chain
Tubulin beta-6 chain	Tubb6	Q922F4	3.05				Cytoskeleton, involved in cell division.
Guanine nucleotide-binding protein G subunit gamma-12	Gng12	Q9DAS9	3.03 ⁻¹				G-protein, signal transduction
Cytochrome c oxidase subunit 6C	Cox6c	Q9CPQ1	3.01 ⁻¹				Mitochondrial respiratory chain
Glycolipid transfer protein	Gltp	Q9JL62	2.75 ⁻¹				Lipid transport
Acyl-CoA-binding protein	Dbi	P31786	2.70 ⁻¹				Lipid metabolism, GABA signal transduction
Leucine zipper transcription factor-like protein 1	Lztfl1	Q9JHQ5	2.63 ⁻¹				Ciliary membrane trafficking, development (sonic hedgehog pathway), neurite outgrowth
Guanine nucleotide-binding protein G subunit gamma-4	Gng4	P50153	2.49 ⁻¹				G-protein, signal transduction
Cytochrome b-c1 complex subunit 7	Uqcrb	Q9D855	2.32 ⁻¹				Mitochondrial respiratory chain
Actin-related protein 2/3 complex subunit 3	Arpc3	Q9JM76	2.29 ⁻¹				Actin polymerization, cell motility
Latrophilin-3	Lphn3	Q80TS3	2.28 ⁻¹				Cell adhesion, synapse formation, axon guidance
Beta-synuclein	Sncb	Q91ZZ3	2.25 ⁻¹				Neuronal plasticity
Cytochrome b-c1 complex subunit 8	Uqcrc	Q9CQ69	2.15 ⁻¹				Mitochondrial respiratory chain
Costars family protein ABRACL	Abrac1	Q4KML4	2.12				Actin-filament based process, cell motility
NADH dehydrogenase [ubiquinone] 1 beta subcomplex subunit 1	Ndufb1	P0DN34	2.02 ⁻¹				Mitochondrial respiratory chain
ProSAAS	Pcsk1n	Q9QXV0		3.95 ⁻¹			Regulation of neuroendocrine secretory pathways
Thymosin beta-4	Tmsb4x	P20065		3.65 ⁻¹			Inhibits Actin polymerization and bone marrow stem cell differentiation
Protein phosphatase 1 regulatory subunit 1A	Ppp1r1a	Q9ERT9		3.33 ⁻¹			Inhibits hormonal control of glycogen metabolism
Dehydrogenase/reductase SDR family member 1	Dhrs1	Q99L04			2.19		Steroid metabolism
Band 3 anion transport protein	Slc4a1	P04919			2.09 ⁻¹		Anion transport across erythrocyte cell membrane
Cystatin-B	Cstb	Q62426			2.05 ⁻¹		Thiol proteinase inhibitor

upregulation during daytime (Figure 2a; Table 4), but were found to be specifically upregulated in nighttime samples of the *Bmal1* CKO neocortex (Figure 4b, Table 5), again seemingly reflecting a loss of protein rhythms in the *Bmal1* CKO cerebral cortex as opposed to a general continuous effect on the proteins themselves. Daytime protein levels were specifically affected for proteins involved in synapse structure (PLXND1 and CAMKV) (Figure 4a, Table 5), whereas an enzyme controlling pH

homeostasis (CA4) was upregulated in both day- and nighttime samples of neocortex of the *Bmal1* CKO mouse.

In addition to the proteins affected across both brain regions described above (FABP7, GFAP, MTHFD1L, ACAA2, and ENTPD2), three proteins (ANXA4, NOS1, and VIM) were found to be differentially expressed between genotypes specifically in the hippocampus, all of which were affected in daytime-samples only (Figure 4c,

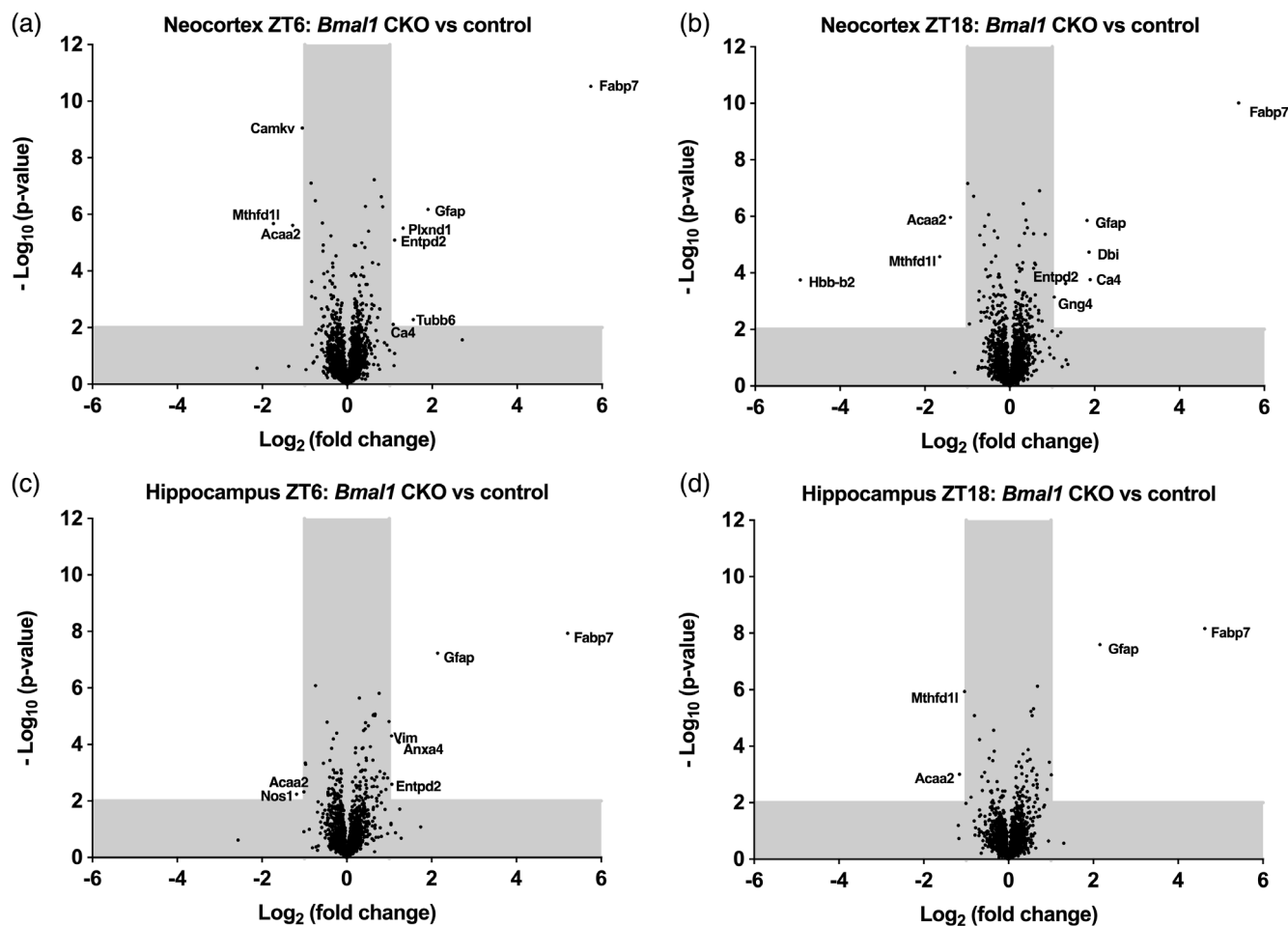


FIGURE 4 *Bmal1* dependent changes in the proteome of the mouse cerebral cortex. Volcano plots of proteomic analyses of differential expression of proteins between the *Bmal1* CKO and control mouse in the neocortex at ZT6 (a), the neocortex at ZT18 (b), the hippocampus at ZT6 (c), and the hippocampus at ZT18 (d). For each identified protein, the negative \log_{10} of the p -value (Student's t -test) is plotted against the \log_2 of the detected fold change calculated as the mean value in the *Bmal1* CKO divided by the mean value in the control. Proteins with $p < .01$ and fold change >2.0 were regarded as being differentially expressed and were included in further analyses (Table 5); shaded areas indicate these cut-off values. $n = 5$ – 8 in each experimental group.

Table 5). These included functionally diverse proteins involved in exocytosis (ANXA4) and nitric oxide synthesis (NOS1), as well as cytoskeletal components (VIM).

3.3 | Transcripts known to be detectable in astrocytes are upregulated in the neocortex and hippocampus of the *Bmal1* CKO mouse

The prominent effect of *Bmal1* deletion on the proteins FABP7 and GFAP, both of which are expressed in astrocytes (Middeldorp & Hol, 2011; Schmid et al., 2006; Sharifi et al., 2011), as well as previous reports on the connection between *Bmal1* and astrocyte biology in other model systems (Lananna et al., 2018; Musiek et al., 2013), prompted us to determine the expression of these proteins in detail at the transcript level both with respect to circadian profiles and genotypical differences. Since

DBI is mainly expressed in astrocytes (Tonon et al., 1990; Tonon et al., 2020), and GNG4 is detectable in fetal astrocytes (Bonham et al., 2018), the transcripts of these proteins, which were both identified as being upregulated in the neocortex of the *Bmal1* CKO mouse (Figures 3b and 4b; Table 5), were also included in the analyses.

To determine circadian profile of *Fabp7*, *Gfap*, *Dbi*, and *Gng4*, qRT-PCR was performed on neocortical and hippocampal samples from the *Bmal1* CKO and control mice collected in 3 h intervals (Figure 5). All four transcripts were significantly upregulated in both cortical areas of the *Bmal1* CKO (p -values $<.01$, two-way ANOVA), whereas circadian rhythms were not detected in either genotype (Table 6). *Fabp7* has been previously shown to exhibit a diurnal rhythm in the mouse hippocampus (Gerstner et al., 2008), and analyzing the expression profile in control mouse separately confirmed these findings with a just significant circadian variation in the hippocampus ($p = .036$, one-way ANOVA) (Figure S4).

TABLE 5 Differential expression of proteins in between genotypes, that is, *Bmal1* CKO versus control, in neocortical and hippocampal samples collected at midnight (ZT18) and midday (ZT6), respectively.

Protein name	Gene symbol	Protein ID	Ratio between <i>Bmal1</i> CKO and control				Function (uniprot.org)
			Neocortex		Hippocampus		
			ZT6	ZT18	ZT6	ZT18	
Fatty acid-binding protein, brain	Fabp7	P51880	53.41	42.07	37.04	24.77	CNS development, establishment of radial glia fibers for neuron migration
Glial fibrillary acidic protein	Gfap	P03995	3.73	3.53	4.43	4.46	Cytoskeleton, cell-specific marker of astrocytes
Monofunctional C1-tetrahydrofolate synthase, mitochondrial	Mthfd1l	Q3V3R1	3.33 ⁻¹	3.15 ⁻¹		2.05 ⁻¹	Mitochondrial metabolite interconversion enzyme
Tubulin beta-6 chain	Tubb6	Q922F4	2.94				Cytoskeleton, involved in cell division.
Plexin-D1	Plxnd1	Q3UH93	2.49				Cell-cell signaling, synapse formation
3-ketoacyl-CoA thiolase, mitochondrial	Acaa2	Q8BWT1	2.43 ⁻¹	2.63 ⁻¹	2.02 ⁻¹	2.05 ⁻¹	Mitochondrial respiratory chain
Ectonucleoside triphosphate diphosphohydrolase 2	Entpd2	O55026	2.17	2.49	2.09		Hydrolyses ATP to regulated purinergic neurotransmission
Carbonic anhydrase 4	Ca4	Q64444	2.12	3.73			Intra- and extracellular pH homeostasis
CaM kinase-like vesicle-associated protein	Camkv	Q3UHL1	2.08 ⁻¹				Dendritic spine maintenance
Hemoglobin subunit beta-2 ^a	Hbb-b2	P02089		30.59 ⁻¹			Oxygen transport
Acyl-CoA-binding protein	Dbi	P31786		3.65			Lipid metabolism, GABA signal transduction
Guanine nucleotide-binding protein G(I)/G(S)/G(O) subunit gamma-4	Gng4	P50153		2.08			G-protein, signal transduction
Annexin A4	Anxa4	P97429			2.35		Exocytosis
Nitric oxide synthase, brain	Nos1	Q9Z0J4			2.27 ⁻¹		Production of nitric oxide (neurotransmitter)
Vimentin	Vim	P20152			2.08		Cytoskeleton, intermediate filament, non-epithelial cells

^aCorrection for possible contamination from blood in the samples was not performed.

The overall transcript levels of *Fabp7* were increased by 18.4-fold and 10.2-fold in the *Bmal1* CKO neocortex and hippocampus, respectively, as compared to controls (Table 6). *Gfap* expression was increased by 3.6-fold in both brain areas, whereas *Dbi* and *Gng4* transcript levels were upregulated by approximately 2.2- and 1.5-fold, respectively (Table 6). An increased abundance of *Fabp7* and *Gfap* transcripts specifically in the cerebral cortex, including both the neocortex and the hippocampus, was also detectable by radiochemical in situ hybridization (Figure 6a-f). The expression levels in the control mouse were close to background with a weak *Gfap* signal detectable only in the white matter of the optic tract, cerebral peduncle, fornix, and internal capsule (Figure 6e). Quantitative analyses of the in situ hybridization signals (Figure 6c,d,g,h) revealed highly significant increases of both *Fabp7* and *Gfap* transcripts in the neocortex and hippocampus of the *Bmal1* CKO mouse as compared to controls (*p*-values <.0001, two-way ANOVA). Thus, the astrocyte proteins identified as being upregulated in the cerebral cortex of the *Bmal1*

CKO mouse in our proteomic analysis are accompanied by increased levels of the corresponding transcripts.

3.4 | GFAP- and FABP7-positive cells are abundant in the cerebral cortex of the *Bmal1* CKO mouse and both proteins colocalize with BMAL1 in the control mouse

To determine the distribution of FABP7- and GFAP-positive cells in the cerebral cortex of the *Bmal1* CKO and to compare it to control mice, immunohistochemistry for detection these proteins was performed on coronal sections of the brains of each genotype (Figure 7). Prominent expression of both proteins was observed in cells with astrocyte morphology in both the neocortex and hippocampus of the *Bmal1* CKO; in the control mice, cells expressing both proteins were seen in the hippocampus, whereas

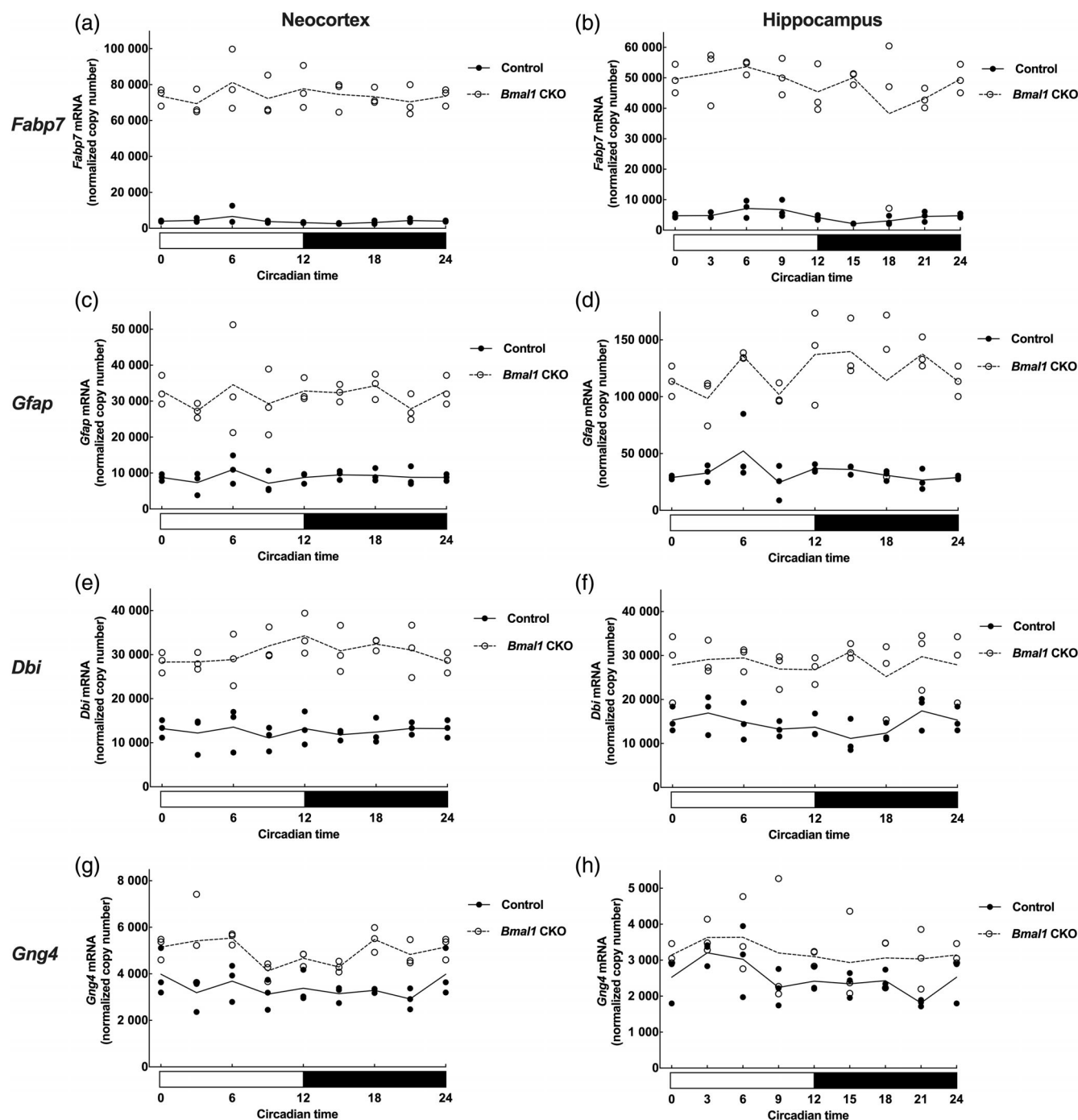


FIGURE 5 Circadian expression profiles of genes expressed in astrocytes in the cerebral cortex of the *Bmal1* CKO and control mice. Quantitative RT-PCR analysis of *Fabp7* in the neocortex (a) and hippocampus (b), *Gfap* in the neocortex (c) and hippocampus (d), *Dbi* in the neocortex (e) and hippocampus (f), and *Gng4* in the neocortex (g) and hippocampus (h). Mice were kept in DD; white and black areas of horizontal bars indicate presumptive day and night, respectively. Data are presented as individual measurements and means for each genotype at each timepoint with open circles-dashed line indicating *Bmal1* CKO genotype and closed circles-solid line indicating control. Data from circadian time (CT) 0/CT24 are double plotted. $n = 3$ in each experimental group. Statistical analyses are presented in Table 6.

few positive cells were detectable in the neocortex. Cellular colocalization of FABP7 and GFAP was evident in both the neocortex and hippocampus of the *Bmal1* CKO (Figure 7), suggesting that FABP7 is expressed in astrocytes of the cerebral cortex of the *Bmal1* CKO.

Semiquantitative analyses of GFAP-immunopositive cells in the neocortex and hippocampus of both genotypes (Figure 7b) revealed a significantly higher abundance of GFAP-positive cells in both the neocortex ($p = .029$, Mann-Whitney U-test) and the hippocampus ($p = .029$, Mann-Whitney U-test). In the hippocampus, the

TABLE 6 Summary of quantitative analyses of the expression profiles of *Fabp7*, *Gfap*, *Dbi*, and *Gng4* in the neocortex and hippocampus of the *Bmal1* CKO and the control mouse determined by qRT-PCR.

Transcript	Brain area	Genotype	Difference between genotypes (p-value + significance level) ^a	Circadian changes (significance level)	Expression level (mean ± SEM) ^b	Fold change between genotypes (ratio ± SE) ^c
<i>Fabp7</i>	Neocortex	<i>Arntl</i> CKO	<.0001****	ns	74063.1 (±1366.5)	18.4 (±2.0)
		Control		ns	4034.41 (±428.0)	
<i>Gfap</i>		<i>Arntl</i> CKO	<.0001****	ns	31422.2 (±1005.2)	3.6 (±0.2)
		Control		ns	8847.7 (±427.1)	
<i>Dbi</i>		<i>Arntl</i> CKO	<.0001****	ns	30785.8 (±756.7)	2.4 (±0.1)
		Control		ns	12600.5 (±304.1)	
<i>Gng4</i>		<i>Arntl</i> CKO	<.0001****	ns	4939.3 (±192.6)	1.5 (±0.1)
		Control		ns	3342.6 (±120.9)	
<i>Fabp7</i>	Hippocampus	<i>Arntl</i> CKO	<.0001****	ns	47742.5 (±1795.5)	10.2 (±1.4)
		Control		ns	4666.4 (±592.8)	
<i>Gfap</i>		<i>Arntl</i> CKO	<.0001****	ns	122299.7 (±6070.4)	3.6 (±0.4)
		Control		ns	33624.0 (±3059.0)	
<i>Dbi</i>		<i>Arntl</i> CKO	<.0001****	ns	28247.1 (±665.75)	2.0 (±0.1)
		Control		ns	14376.9 (±766.2)	
<i>Gng4</i>		<i>Arntl</i> CKO	.0032**	ns	3219.6 (±94.9)	1.3 (±0.1)
		Control		ns	2502.2 (±155.4)	

^aDifference between genotypes and circadian changes were determined by two-way ANOVA followed by Bonferroni's multiple comparisons post hoc tests.

^bGene expression levels were determined by calculating the overall mean of the mean values at each timepoint analyzed.

^cFold change between genotypes was determined as the ratio between the overall mean values of the *Bmal1* CKO and the control mouse from the same brain area.

increased number of GFAP-positive cells was accompanied by an increased level of GFAP immunoreactivity in individual cells ($p = .0017$, Student's *t*-test), whereas a significant difference in GFAP signal intensities between genotypes was not detected in the neocortex ($p = .096$, Student's *t*-test). These findings suggest that the increased level of GFAP in the cerebral cortex of the *Bmal1* CKO revealed by our proteomic analysis reflects an increased number of cells expressing the protein at detectable levels and partly an increased expression in individual cells. Notably, similar semiquantitative analyses of sections immunoreacted for detection of cell-type specific markers of oligodendrocytes (Bin et al., 2016), microglia (Boeck et al., 2020), and neurons (Mullen et al., 1992) did not reveal differences between genotypes in cell numbers in the neocortex and hippocampus (Figure S5). These findings are in accord with the our proteomic analyses which did not identify genotype-dependent

differences in any of the detected molecular markers (Matson et al., 2022; Russ et al., 2021) of neurons, microglia, or oligodendrocytes, including oligodendrocyte precursor cells (Table S9).

BMAL1 is known to be expressed in neurons of the murine neocortex and hippocampus (Rath et al., 2014); however, FABP7, which is upregulated in the *Bmal1* CKO, did not colocalize with the neuronal marker NeuN (Figure S6). Therefore, to establish if BMAL1 was also present in cortical astrocytes expressing GFAP and FABP7, immunohistochemical staining were performed on sections of control mice (Figure 8). In both the neocortex and the hippocampus, cells expressing both BMAL1, GFAP and FABP7 were identified, suggesting that intrinsic BMAL1 can influence the biology of individual cortical astrocytes. Notably, BMAL1 was undetectable in astrocytes in the neocortex and hippocampus of the *Bmal1* CKO mouse (Figure S7).

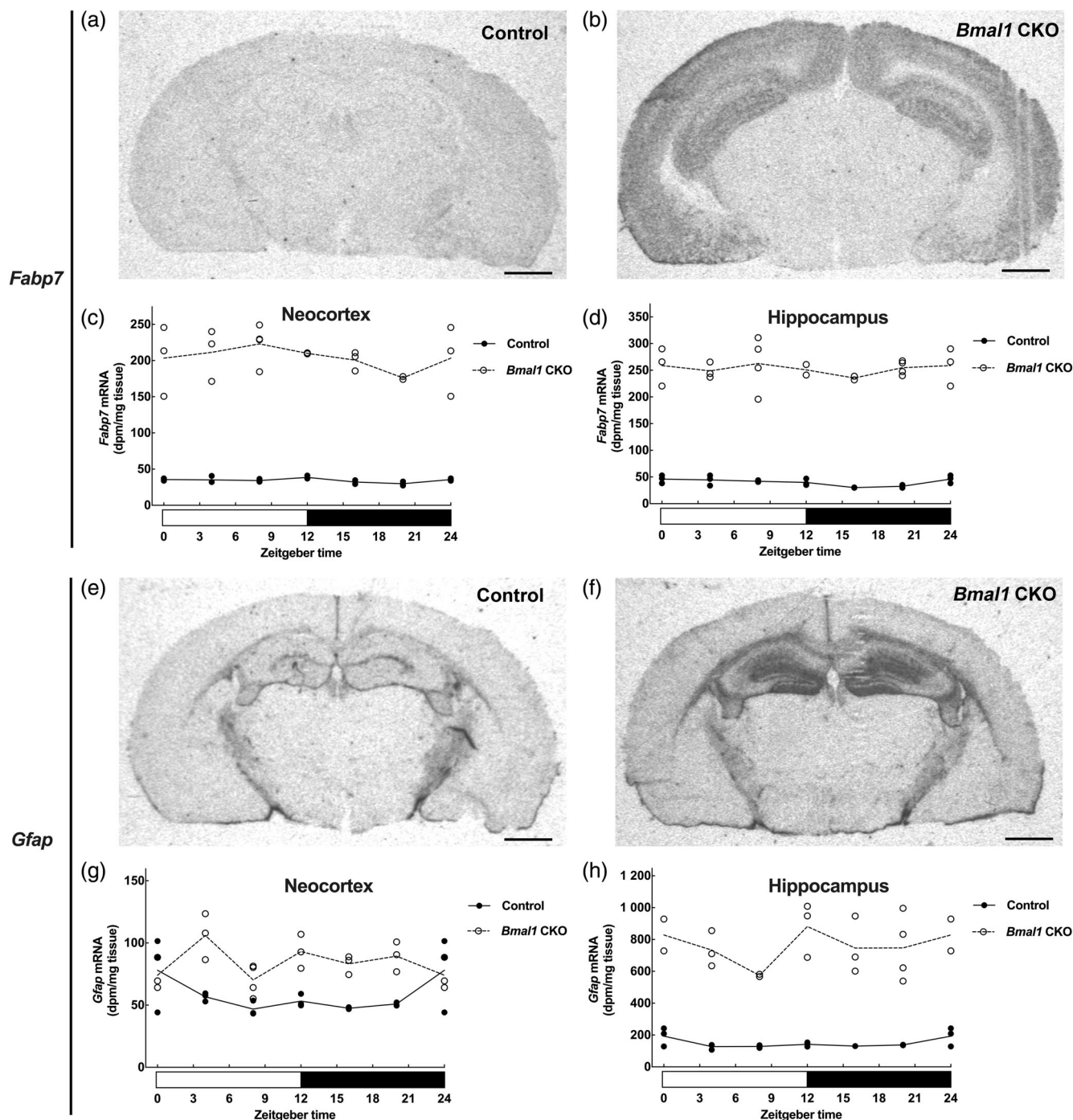


FIGURE 6 Daily expression and distribution of *Fabp7* and *Gfap* transcripts in the cerebral cortex of control and *Bmal1* CKO mice. (a–d) Radiochemical in situ hybridization for detection of *Fabp7* transcripts with representative autoradiographs (ZT12) of the control mouse (a) and the *Bmal1* CKO mouse (b) and semiquantitative analyses of expression levels in the neocortex (c) and the hippocampus (d) during the 24 h LD cycle. (e–h) Radiochemical in situ hybridization for detection of *Gfap* transcripts with representative autoradiographs (ZT12) of the control mouse (e) and the *Bmal1* CKO mouse (f) and semiquantitative analyses of expression levels in the neocortex (g) and the hippocampus (h) during the 24 h LD cycle. White and black areas of horizontal bars indicate day and night, respectively. Data are presented as individual measurements and means for each genotype at each timepoint with open circles-dashed line indicating *Bmal1* CKO genotype and closed circles-solid line indicating control. Data from ZT0/ZT24 are double plotted. Genotypes were compared by two-way ANOVA showing significant highly differences for both genes analyzed (p -values < .0001). $n = 2$ –4 in each experimental group. Scale bars, 1 mm.

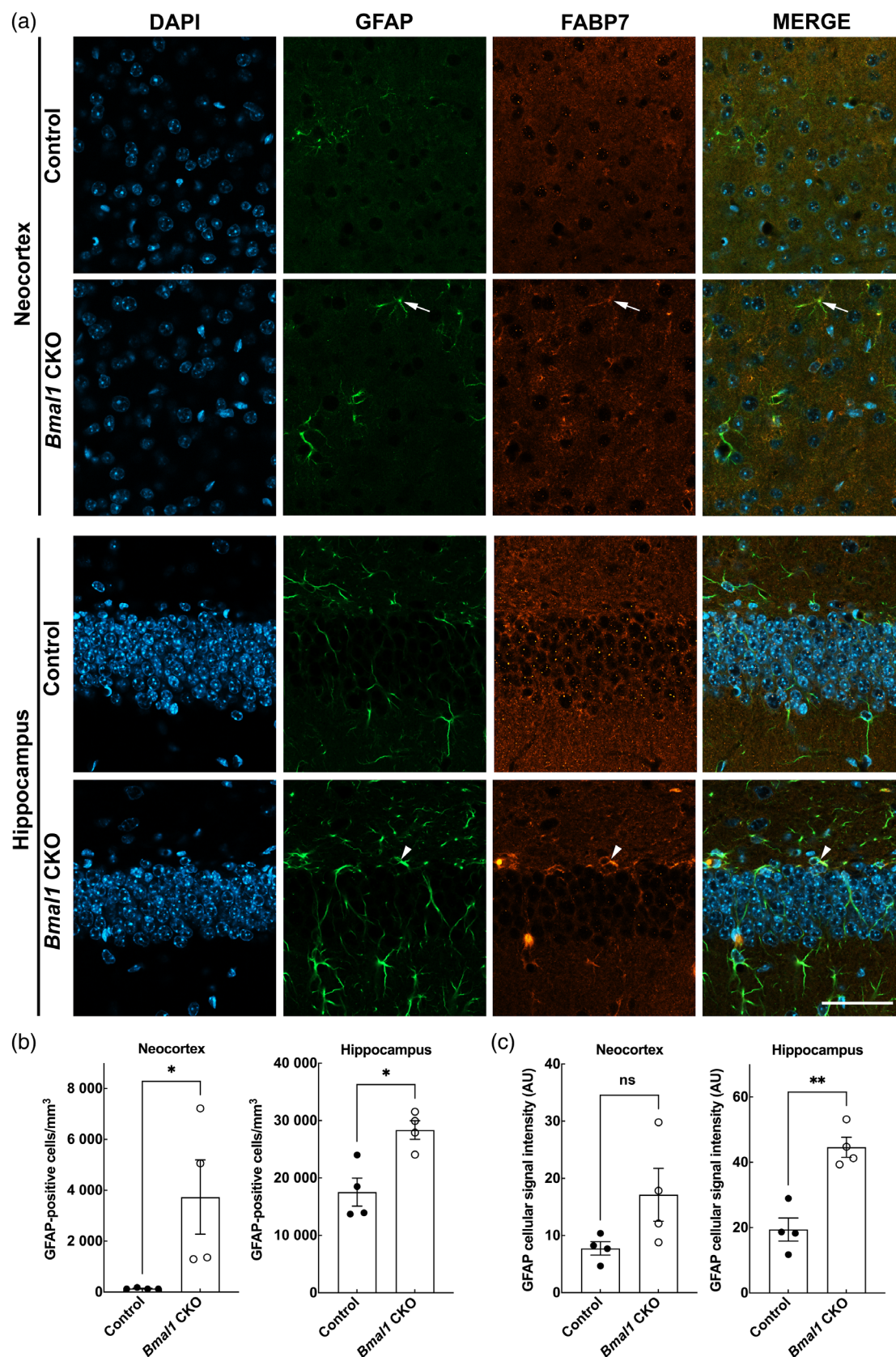


FIGURE 7 Legend on next page.

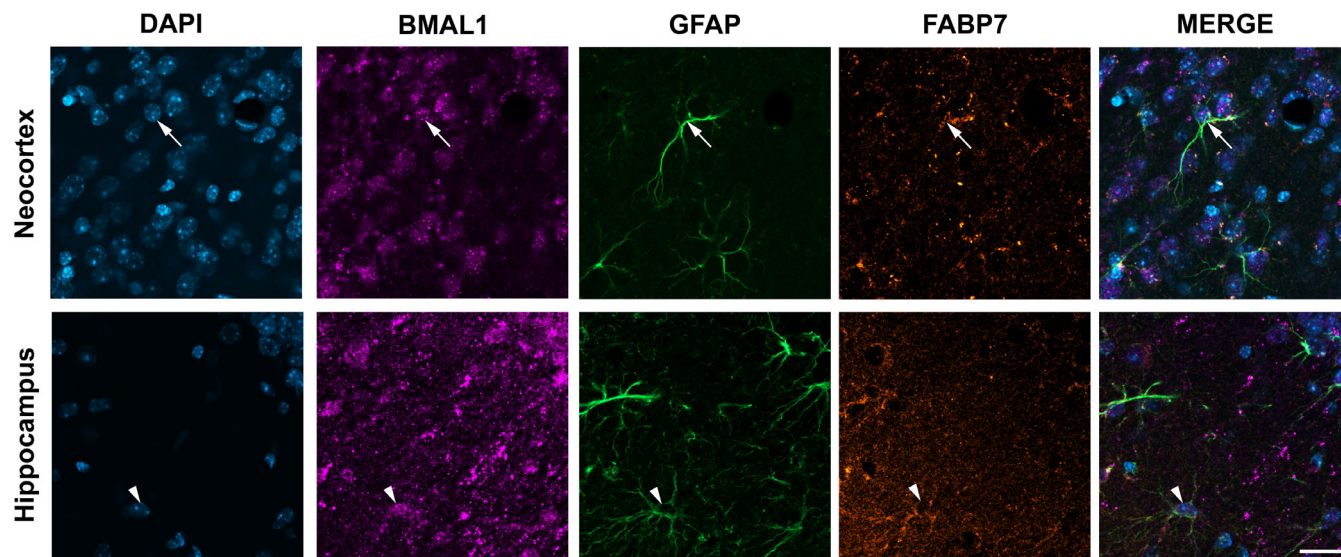


FIGURE 8 Colocalization of BMAL1, FABP7, and GFAP in the neocortex and hippocampus of the control mouse. Immunohistochemistry for detection of BMAL1, GFAP, and FABP7 was performed on the same sections. Colocalization of all three proteins were detected in astrocytes of the neocortex (arrows) and the hippocampus (arrow heads). Images of the second layer of the neocortex and the dentate gyrus are displayed. $n = 3$. Scale bar, 50 μm .

4 | DISCUSSION

The cerebral cortex contains a circadian oscillator as evidenced by rhythmic expression of clock genes in both the neocortex and the hippocampus (Jilg et al., 2010; Rath et al., 2014). We here identified proteins differentially expressed between day and night in the neocortex and hippocampus of the mouse and further determined downstream targets of the cortical circadian oscillator by proteomic analysis of a cerebral cortex-specific *Bmal1* clock gene knockout mouse.

In the current study, 15 day-night differentially expressed proteins were identified in the neocortex, while only three were identified in the hippocampus, indicating that the hippocampus is generally less rhythmic than the neocortex, as also seen in analyses of clock gene expression profiles in the mouse, where the amplitude is higher in neocortex as compared to the hippocampus (Bering et al., 2018). In the mouse neocortex, a number of mitochondrial respiratory chain proteins were upregulated during daytime. Enrichment of mitochondrial respiratory chain proteins has also been reported in the rhythmic proteome of the mouse SCN, in which the respiratory chain proteins were mainly upregulated during daytime (Chiang et al., 2014). In the cerebellum, a pattern with upregulation during daytime is also in agreement with our data, although other mitochondrial respiratory

chain components were identified as being rhythmic (Plumel et al., 2019). In the liver, proteins of the mitochondrial respiratory chain are also rhythmic, but the rhythms are more complex in that individual components are not uniformly distributed across the 24 h cycle and are not synchronized to the neocortical proteins identified in the current study (Neufeld-Cohen et al., 2016). Previous proteomic day-night analyses of the rat pineal gland also identified mitochondrial proteins, including one mitochondrial respiratory chain protein, as being preferentially expressed during daytime (Moller et al., 2007), but this was not the case in a similar analysis of the mouse retina (Moller et al., 2017).

In the neocortex, we also identified a number of rhythmic neuroplasticity proteins upregulated during daytime. Studies on time of day-dependent neurogenesis and plasticity of the adult brain has mostly focused the hippocampus and its role in learning and memory (Ali & von Gall, 2022; Snider et al., 2018), whereas little is known about the diurnal neuroplasticity processes in the mature neocortex (Maret et al., 2011). In this regard, our data may represent a first step towards identifying the molecular basis for circadian regulation of neocortical plasticity.

Clock gene-encoded proteins were not detected in our proteomic analyses, probably reflecting that expression levels are too low to

FIGURE 7 Distribution of FABP7 and GFAP protein and semiquantitative analyses of GFAP in the neocortex and hippocampus of *Bmal1* CKO and control mice. (a) Immunohistochemical stainings for both GFAP and FABP7 were performed on the same sections. DAPI staining is shown for orientations purposes; microphotographs of the second cortical layer and the dentate gyrus are displayed. Examples on colocalization of GFAP and FABP7 in astrocytes in the *Bmal1* CKO mouse are indicated by arrows in the neocortex and arrow heads in hippocampus, respectively. $n = 3$ –4 in each experimental group. Scale bar, 50 μm . (b) GFAP-positive cells were counted in the neocortex and the hippocampus of control mice (closed circles) and *Bmal1* CKO mice (open circles). Data analyzed by Mann–Whitney U-test with $n = 4$ in each experimental group. $*p < .05$. (c) GFAP signal intensity was measured in the neocortex and the hippocampus of control mice (closed circles) and *Bmal1* CKO mice (open circles). Data analyzed by Student's *t*-test with $n = 4$ in each experimental group. $**p < .01$; ns, not significant.



generate a significant protein signal. As described in the introduction, immunohistochemical analyses have identified clock gene-encoded proteins in the cerebral cortex, and large screening efforts at the transcript level also reported rhythmic clock gene expression in the cerebral cortex (Renaud et al., 2015). This apparent discrepancy seems to reflect a limitation of the methodology; thus, even in the pineal gland, a central structure in circadian biology, proteomic analyses in the rat failed to identify clock gene-encoded protein products (Moller et al., 2007), while the corresponding transcripts were detected by microarray analysis (Bailey et al., 2009). Most importantly, the local circadian oscillator of the neocortex seems to play a key-role in governing differential day-night expression of proteins, as evidenced by the marked decline in the number of day-night differentially expressed proteins in the *Bmal1* deficient neocortex in the current study.

Apart from the reduced representation of rhythmic proteins, a striking feature of the proteome of the *Bmal1* CKO is the upregulation of proteins known to be expressed in astrocytes. FABP7, which is expressed in neural stem cells and radial glia, but seems to persist in astrocytes and oligodendrocytes precursors of the adult brain (Kipp et al., 2011; Schmid et al., 2006; Sharifi et al., 2011), was upregulated by more than tenfold in both the hippocampus and neocortex at both transcript and protein level in the *Bmal1* CKO. Upregulation of GFAP, a well-established astrocyte marker (Middeldorp & Hol, 2011), was fourfold, but this protein still represents the second highest level of differential expression between genotypes in both brain regions. Our finding that BMAL1, FABP7, and GFAP are co-expressed in astrocytes of the neocortex and hippocampus of control mice suggests that BMAL1 may act locally in cortical astrocytes to repress activation. These results support activation of astrocytes as a general feature of CNS model systems with knockout of *Bmal1*, since a modest upregulation of *Fabp7* transcripts in the hypothalamus of global *Bmal1* knockout mice was recently reported (Gerstner & Paschos, 2020), whereas the relation between a knockout of BMAL1 and activation of GFAP-positive astrocyte has been previously reported both in vitro and in vivo (Lananna et al., 2018; Musiek et al., 2013).

Despite the apparent connection of GFAP to the circadian clock, GFAP is not rhythmic in the mouse SCN (Moriya et al., 2000) and although day-night differences have been reported in the rat SCN (Gerics et al., 2006; Hajos, 2008), our data establish the non-rhythmic nature *Gfap* expression in both the neocortex and the hippocampus of the mouse. Despite a rhythm in the hippocampus as reported here and elsewhere (Gerstner et al., 2008), neocortical *Fabp7* is also continuously expressed throughout the 24 h circadian cycle in the neocortex. Thus, the clear connection of *Gfap* and *Fabp7* to the circadian clock is not necessarily translated into a down-stream circadian rhythm. Clock-dependent mechanisms involving activation of astrocytes, as reflected by the upregulation of GFAP and FABP7, seem to play a key-role in neurotoxicity and neurodegenerative diseases (Killooy et al., 2020; Musiek & Holtzman, 2016), which may in turn induce the depressive phenotype of the *Bmal1* CKO.

Our proteomic analyses expanded the list of *Bmal1*-regulated astrocytic proteins (Gerstner & Paschos, 2020; Lananna et al., 2018; Musiek et al., 2013) to include GNG4 and DBI (Bonham et al., 2018; Tonon

et al., 1990); in addition to the increase caused by deletion of *Bmal1*, both of these proteins were found to be upregulated at night in the proteomic analysis of the control neocortex, but did not display a circadian rhythm at the transcript level, suggesting that rhythms are regulated at the posttranscriptional level. ENTPD2, a protein identified as being upregulated in our proteomic analysis of the *Bmal1* CKO cerebral cortex, has also been identified in rat astrocytes (Wink et al., 2006), and VIM, another protein upregulated specifically in the hippocampus of the *Bmal1* CKO, has also been localized to astrocytes (Schnitzer et al., 1981), which is in accord with our finding of an increased abundance of GFAP-positive astrocytes in both the hippocampus and neocortex of the *Bmal1* CKO mouse. On the other hand, previous investigations found that FABP7 is downregulated in the cerebellum of *Per1/Per2* global mutant mice (Plumel et al., 2019), whereas *Gfap* expression seems to be unaffected in the cerebral cortex (Lananna et al., 2018). Therefore, the marked upregulation of astrocyte markers following *Bmal1* knockout does not seem to be a general consequence of interfering with the molecular circadian clock.

In the *Bmal1* CKO mouse model, we have previously documented depressive-like symptoms (Bering et al., 2018), and now we see a correlation with increased astrocyte activity specifically in the hippocampus and the neocortex. On the contrary, the general picture in humans diagnosed with major depressive disorder seems to be a reduction in astrocyte density in the cerebral cortex (Cobb et al., 2016; O'Leary et al., 2021; Rajkowska & Stockmeier, 2013), but astrocyte hypertrophy has also been reported (Torres-Platas et al., 2011); this points to the possibility that dysregulation rather than absolute levels of cortical astrocyte activity and density may induce a depressive phenotype. Recent data suggest that disruption of cortical astrocyte calcium-signaling induces a depressive-like behavior accompanied by synaptic structure abnormalities in mice (Luo et al., 2023), which may be part of the mechanistic explanation linking astrocytes to depression. Another CKO mouse model, generated by use of a Cre-construct driven by the *CamKII*-promoter to knock out *Bmal1* in all regions of the forebrain, while cellularly limiting the deletion to excitatory neurons, did not exhibit any affective symptoms (Snider et al., 2016). This indicates that the depressive-like behavior observed in the phenotypic characterization of the mouse analyzed in the current study (Bering et al., 2018) is not caused by *Bmal1* deletion in these neurons. On the other hand, *Emx1* which was driving the Cre used to knock out *Bmal1* is known to be expressed in neurons, including excitatory neurons, and astrocyte precursors of the developing cerebral cortex (Gorski et al., 2002). Therefore, we speculate that the cellular distribution of the *Bmal1* knockout, including astrocytes, may be a defining feature of the reported differences between the behavioral phenotypes of the two otherwise seemingly similar mouse models (Bering et al., 2018; Snider et al., 2016), again supporting the interpretation that malfunction of cortical *Bmal1*-positive astrocytes represents a step towards a depressive-like phenotype.

AUTHOR CONTRIBUTIONS

Bent Honoré and Martin Fredensborg Rath conceived the study. Tenna Bering, Bent Honoré, and Martin Fredensborg Rath designed experiments. Tenna Bering, Camilla Gadgaard, Bent

Honoré, and Martin Fredensborg Rath performed experiments. Tenna Bering, Camilla Gadgaard, Henrik Vorum, Bent Honoré, and Martin Fredensborg Rath analyzed data. Martin Fredensborg Rath wrote the manuscript. Tenna Bering, Henrik Vorum, and Bent Honoré revised the manuscript. All authors approved the final manuscript.

ACKNOWLEDGMENTS

The authors wish to thank Hanne Kidmose (Department of Biomedicine, University of Aarhus), Rikke Lundorf (Department of Neuroscience, University of Copenhagen), and Dr. Pablo Hernández-Varas (Core Facility for Integrated Microscopy, University of Copenhagen) for expert technical assistance.

FUNDING INFORMATION

This study was supported by the Lundbeck Foundation (grant numbers R108-A10301 and R344-2020-261 to Martin Fredensborg Rath), Independent Research Fund Denmark (grant number 1030-00045B to Martin Fredensborg Rath), the Novo Nordisk Foundation (grant number NNF21OC0070214 to Martin Fredensborg Rath), and Læge Sofus Carl Emil Friis og hustru Olga Doris Friis' Legat (to Martin Fredensborg Rath). The mass spectrometry platform was funded by A.P. Møller og Hustru Chastine McKinney Møllers Fond til Almene Formaal.

CONFLICT OF INTEREST STATEMENT

The authors declare no conflicts of interest.

DATA AVAILABILITY STATEMENT

The data that support the findings of this study are available from the corresponding author upon reasonable request.

ORCID

Tenna Bering  <https://orcid.org/0000-0003-2049-4792>

Camilla Gadgaard  <https://orcid.org/0000-0002-7514-6325>

Henrik Vorum  <https://orcid.org/0000-0002-7600-0731>

Bent Honoré  <https://orcid.org/0000-0002-3459-7429>

Martin Fredensborg Rath  <https://orcid.org/0000-0002-4047-6324>

REFERENCES

- Ali, A. A. H., & von Gall, C. (2022). Adult neurogenesis under control of the circadian system. *Cells*, 11(5), 764. <https://doi.org/10.3390/cells11050764>
- Bailey, M. J., Coon, S. L., Carter, D. A., Humphries, A., Kim, J. S., Shi, Q., Gaildrat, P., Morin, F., Ganguly, S., Hogenesch, J. B., Weller, J. L., Rath, M. F., Moller, M., Baler, R., Sugden, D., Rangel, Z. G., Munson, P. J., & Klein, D. C. (2009). Night/day changes in pineal expression of >600 genes: Central role of adrenergic/cAMP signaling. *The Journal of Biological Chemistry*, 284(12), 7606–7622. <https://doi.org/10.1074/jbc.M808394200>
- Bering, T., Carstensen, M. B., & Rath, M. F. (2017). Deleting the Arntl clock gene in the granular layer of the mouse cerebellum: Impact on the molecular circadian clockwork. *Journal of Neurochemistry*, 142(6), 841–856. <https://doi.org/10.1111/jnc.14128>
- Bering, T., Carstensen, M. B., Wortwein, G., Weikop, P., & Rath, M. F. (2018). The circadian oscillator of the cerebral cortex: Molecular, biochemical and behavioral effects of deleting the Arntl clock Gene in cortical neurons. *Cerebral Cortex*, 28(2), 644–657. <https://doi.org/10.1093/cercor/bhw406>
- Bin, J. M., Harris, S. N., & Kennedy, T. E. (2016). The oligodendrocyte-specific antibody 'CC1' binds quaking 7. *Journal of Neurochemistry*, 139(2), 181–186. <https://doi.org/10.1111/jnc.13745>
- Boeck, M., Thien, A., Wolf, J., Hagemeyer, N., Laich, Y., Yusuf, D., Backofen, R., Zhang, P., Boneva, S., Stahl, A., Hilgendorf, I., Agostini, H., Prinz, M., Wieghofer, P., Schlunck, G., Schlecht, A., & Lange, C. (2020). Temporospatial distribution and transcriptional profile of retinal microglia in the oxygen-induced retinopathy mouse model. *Glia*, 68(9), 1859–1873. <https://doi.org/10.1002/glia.23810>
- Bonham, L. W., Evans, D. S., Liu, Y., Cummings, S. R., Yaffe, K., & Yokoyama, J. S. (2018). Neurotransmitter pathway genes in cognitive decline during aging: Evidence for GNG4 and KCNQ2 genes. *American Journal of Alzheimer's Disease and Other Dementias*, 33(3), 153–165. <https://doi.org/10.1177/1533317517739384>
- Chiang, C. K., Mehta, N., Patel, A., Zhang, P., Ning, Z., Mayne, J., Sun, W. Y., Cheng, H. Y., & Figeys, D. (2014). The proteomic landscape of the suprachiasmatic nucleus clock reveals large-scale coordination of key biological processes. *PLoS Genetics*, 10(10), e1004695. <https://doi.org/10.1371/journal.pgen.1004695>
- Cobb, J. A., O'Neill, K., Milner, J., Mahajan, G. J., Lawrence, T. J., May, W. L., Miguel-Hidalgo, J., Rajkowska, G., & Stockmeier, C. A. (2016). Density of GFAP-immunoreactive astrocytes is decreased in left hippocampi in major depressive disorder. *Neuroscience*, 316, 209–220. <https://doi.org/10.1016/j.neuroscience.2015.12.044>
- Foerster, S., Guzman de la Fuente, A., Kagawa, Y., Bartels, T., Owada, Y., & Franklin, R. J. M. (2020). The fatty acid binding protein FABP7 is required for optimal oligodendrocyte differentiation during myelination but not during remyelination. *Glia*, 68(7), 1410–1420. <https://doi.org/10.1002/glia.23789>
- Gampe, K., Stefani, J., Hammer, K., Brendel, P., Potzsch, A., Enikolopov, G., Enyaji, K., Acker-Palmer, A., Robson, S. C., & Zimmermann, H. (2015). NTPDase2 and purinergic signaling control progenitor cell proliferation in neurogenic niches of the adult mouse brain. *Stem Cells*, 33(1), 253–264. <https://doi.org/10.1002/stem.1846>
- Geric, B., Szalay, F., & Hajos, F. (2006). Glial fibrillary acidic protein immunoreactivity in the rat suprachiasmatic nucleus: Circadian changes and their seasonal dependence. *Journal of Anatomy*, 209(2), 231–237. <https://doi.org/10.1111/j.1469-7580.2006.00593.x>
- Gerstner, J. R., Bremer, Q. Z., Vander Heyden, W. M., Lavaute, T. M., Yin, J. C., & Landry, C. F. (2008). Brain fatty acid binding protein (Fabp7) is diurnally regulated in astrocytes and hippocampal granule cell precursors in adult rodent brain. *PLoS One*, 3(2), e1631. <https://doi.org/10.1371/journal.pone.0001631>
- Gerstner, J. R., & Paschos, G. K. (2020). Circadian expression of Fabp7 mRNA is disrupted in Bmal1 KO mice. *Molecular Brain*, 13(1), 26. <https://doi.org/10.1186/s13041-020-00568-7>
- Gorski, J. A., Talley, T., Qiu, M., Puelles, L., Rubenstein, J. L., & Jones, K. R. (2002). Cortical excitatory neurons and glia, but not GABAergic neurons, are produced in the Emx1-expressing lineage. *The Journal of Neuroscience*, 22(15), 6309–6314.
- Guilding, C., & Piggins, H. D. (2007). Challenging the omnipotence of the suprachiasmatic timekeeper: Are circadian oscillators present throughout the mammalian brain? *The European Journal of Neuroscience*, 25(11), 3195–3216. <https://doi.org/10.1111/j.1460-9568.2007.05581.x>
- Guo, H., Hong, S., Jin, X. L., Chen, R. S., Avasthi, P. P., Tu, Y. T., Ivanko, T. L., & Li, Y. (2000). Specificity and efficiency of Cre-mediated recombination in Emx1-Cre knock-in mice. *Biochemical and Biophysical Research Communications*, 273(2), 661–665. <https://doi.org/10.1006/bbrc.2000.2870>
- Hajos, F. (2008). Changes in glial fibrillary acidic protein (GFAP) immunoreactivity reflect neuronal states. *Neurochemical Research*, 33(8), 1643–1650. <https://doi.org/10.1007/s11064-008-9745-2>
- Honma, S., Ikeda, M., Abe, H., Tanahashi, Y., Namiyama, M., Honma, K., & Nomura, M. (1998). Circadian oscillation of BMAL1, a partner of a



- mammalian clock gene clock, in rat suprachiasmatic nucleus. *Biochemical and Biophysical Research Communications*, 250(1), 83–87. <https://doi.org/10.1006/bbrc.1998.9275>
- Hor, C. N., Yeung, J., Jan, M., Emmenegger, Y., Hubbard, J., Xenarios, I., Naef, F., & Franken, P. (2019). Sleep-wake-driven and circadian contributions to daily rhythms in gene expression and chromatin accessibility in the murine cortex. *Proceedings of the National Academy of Sciences of the United States of America*, 116(51), 25773–25783. <https://doi.org/10.1073/pnas.1910590116>
- Jilg, A., Lesny, S., Peruzki, N., Schwegler, H., Selbach, O., Dehghani, F., & Stehle, J. H. (2010). Temporal dynamics of mouse hippocampal clock gene expression support memory processing. *Hippocampus*, 20(3), 377–388. <https://doi.org/10.1002/hipo.20637>
- Killoy, K. M., Harlan, B. A., Pehar, M., & Vargas, M. R. (2020). FABP7 upregulation induces a neurotoxic phenotype in astrocytes. *Glia*, 68(12), 2693–2704. <https://doi.org/10.1002/glia.23879>
- Kipp, M., Clarner, T., Gingele, S., Pott, F., Amor, S., van der Valk, P., & Beyer, C. (2011). Brain lipid binding protein (FABP7) as modulator of astrocyte function. *Physiological Research*, 60(1), S49–S60. <https://doi.org/10.33549/physiolres.932168>
- Lananna, B. V., Nadarajah, C. J., Izumo, M., Cedeno, M. R., Xiong, D. D., Dimitry, J., Tso, C. F., McKee, C. A., Griffin, P., Sheehan, P. W., Haspel, J. A., Barres, B. A., Liddel, S. A., Takahashi, J. S., Karatsoreos, I. N., & Musiek, E. S. (2018). Cell-autonomous regulation of astrocyte activation by the circadian clock protein BMAL1. *Cell Reports*, 25(1), 1–9.e5. <https://doi.org/10.1016/j.celrep.2018.09.015>
- Li, J. Z., Bunney, B. G., Meng, F., Hagenauer, M. H., Walsh, D. M., Vawter, M. P., Evans, S. J., Choudary, P. V., Cartagena, P., Barchas, J. D., Schatzberg, A. F., Jones, E. G., Myers, R. M., Watson, S. J., Jr., Akil, H., & Bunney, W. E. (2013). Circadian patterns of gene expression in the human brain and disruption in major depressive disorder. *Proceedings of the National Academy of Sciences of the United States of America*, 110(24), 9950–9955. <https://doi.org/10.1073/pnas.1305814110>
- Logan, R. W., & McClung, C. A. (2019). Rhythms of life: Circadian disruption and brain disorders across the lifespan. *Nature Reviews. Neuroscience*, 20(1), 49–65. <https://doi.org/10.1038/s41583-018-0088-y>
- Ludvigsen, M., Thorlacius-Ussing, L., Vorum, H., Moyer, M. P., Stender, M. T., Thorlacius-Ussing, O., & Honore, B. (2020). Proteomic characterization of colorectal cancer cells versus Normal-derived colon mucosa cells: Approaching identification of novel diagnostic protein biomarkers in colorectal cancer. *International Journal of Molecular Sciences*, 21(10), 3466. <https://doi.org/10.3390/ijms21103466>
- Luo, R., Zhou, B., Liao, P., Zuo, Y., & Jiang, R. (2023). Disrupting cortical astrocyte Ca(2+) signaling in developing brain induces social deficits and depressive-like behaviors. *Glia*, 71, 1592–1606. <https://doi.org/10.1002/glia.24358>
- Maret, S., Faraguna, U., Nelson, A. B., Cirelli, C., & Tononi, G. (2011). Sleep and waking modulate spine turnover in the adolescent mouse cortex. *Nature Neuroscience*, 14(11), 1418–1420. <https://doi.org/10.1038/nn.2934>
- Matson, K. J. E., Russ, D. E., Kathe, C., Hua, I., Maric, D., Ding, Y., Krynskiy, J., Pursley, R., Sathyamurthy, A., Squair, J. W., Levi, B. P., Courtine, G., & Levine, A. J. (2022). Single cell atlas of spinal cord injury in mice reveals a pro-regenerative signature in spinocerebellar neurons. *Nature Communications*, 13(1), 5628. <https://doi.org/10.1038/s41467-022-33184-1>
- Middeldorp, J., & Hol, E. M. (2011). GFAP in health and disease. *Progress in Neurobiology*, 93(3), 421–443. <https://doi.org/10.1016/j.pneurobio.2011.01.005>
- Moller, M., Rath, M. F., Ludvigsen, M., Honore, B., & Vorum, H. (2017). Diurnal expression of proteins in the retina of the blind cone-rod homeobox (Crx(−/−)) mouse and the 129/Sv mouse: A proteomic study. *Acta Ophthalmologica*, 95(7), 717–726. <https://doi.org/10.1111/aos.13429>
- Moller, M., Sparre, T., Bache, N., Roepstorff, P., & Vorum, H. (2007). Proteomic analysis of day-night variations in protein levels in the rat pineal gland. *Proteomics*, 7(12), 2009–2018. <https://doi.org/10.1002/pmic.200600963>
- Moriya, T., Yoshinobu, Y., Kouzu, Y., Katoh, A., Gomi, H., Ikeda, M., Yoshioka, T., Itohara, S., & Shibata, S. (2000). Involvement of glial fibrillary acidic protein (GFAP) expressed in astroglial cells in circadian rhythm under constant lighting conditions in mice. *Journal of Neuroscience Research*, 60(2), 212–218.
- Mullen, R. J., Buck, C. R., & Smith, A. M. (1992). NeuN, a neuronal specific nuclear protein in vertebrates. *Development*, 116(1), 201–211. <https://doi.org/10.1242/dev.116.1.201>
- Musiek, E. S., & Holtzman, D. M. (2016). Mechanisms linking circadian clocks, sleep, and neurodegeneration. *Science*, 354(6315), 1004–1008. <https://doi.org/10.1126/science.aah4968>
- Musiek, E. S., Lim, M. M., Yang, G., Bauer, A. Q., Qi, L., Lee, Y., Roh, J. H., Ortiz-Gonzalez, X., Dearborn, J. T., Culver, J. P., Herzog, E. D., Hogenesch, J. B., Wozniak, D. F., Dikranian, K., Giasson, B. I., Weaver, D. R., Holtzman, D. M., & Fitzgerald, G. A. (2013). Circadian clock proteins regulate neuronal redox homeostasis and neurodegeneration. *The Journal of Clinical Investigation*, 123(12), 5389–5400. <https://doi.org/10.1172/JCI70317>
- Neufeld-Cohen, A., Robles, M. S., Aviram, R., Manella, G., Adamovich, Y., Ladeux, B., Nir, D., Rousoo-Noori, L., Kuperman, Y., Golik, M., Mann, M., & Asher, G. (2016). Circadian control of oscillations in mitochondrial rate-limiting enzymes and nutrient utilization by PERIOD proteins. *Proceedings of the National Academy of Sciences of the United States of America*, 113(12), E1673–E1682. <https://doi.org/10.1073/pnas.1519650113>
- O'Leary, L. A., Belliveau, C., Davoli, M. A., Ma, J. C., Tanti, A., Turecki, G., & Mechawar, N. (2021). Widespread decrease of cerebral vimentin-immunoreactive astrocytes in depressed suicides. *Frontiers in Psychiatry*, 12, 640963. <https://doi.org/10.3389/fpsy.2021.640963>
- Plumel, M., Dumont, S., Maes, P., Sandu, C., Felder-Schmittbuhl, M. P., Challet, E., & Bertile, F. (2019). Circadian analysis of the mouse cerebellum proteome. *International Journal of Molecular Sciences*, 20(8), 1852. <https://doi.org/10.3390/ijms20081852>
- Rajkowska, G., & Stockmeier, C. A. (2013). Astrocyte pathology in major depressive disorder: Insights from human postmortem brain tissue. *Current Drug Targets*, 14(11), 1225–1236. <https://doi.org/10.2174/13894501113149990156>
- Rath, M. F., & Moller, M. (2022). Radiochemical In situ hybridization in developmental studies of the pineal gland. *Methods in Molecular Biology*, 2550, 75–84. https://doi.org/10.1007/978-1-0716-2593-4_10
- Rath, M. F., Rohde, K., Fahrenkrug, J., & Moller, M. (2013). Circadian clock components in the rat neocortex: Daily dynamics, localization and regulation. *Brain Structure & Function*, 218(2), 551–562. <https://doi.org/10.1007/s00429-012-0415-4>
- Rath, M. F., Rovsing, L., & Moller, M. (2014). Circadian oscillators in the mouse brain: Molecular clock components in the neocortex and cerebellar cortex. *Cell and Tissue Research*, 357(3), 743–755. <https://doi.org/10.1007/s00441-014-1878-9>
- Renaud, J., Dumont, F., Khelfaoui, M., Foisset, S. R., Letourneur, F., Bienvenu, T., Khwaja, O., Dorsey, O., & Billuart, P. (2015). Identification of intellectual disability genes showing circadian clock-dependent expression in the mouse hippocampus. *Neuroscience*, 308, 11–50. <https://doi.org/10.1016/j.neuroscience.2015.08.066>
- Russ, D. E., Cross, R. B. P., Li, L., Koch, S. C., Matson, K. J. E., Yadav, A., Alkaslasi, M. R., Lee, D. I., Le Pichon, C. E., Menon, V., & Levine, A. J. (2021). A harmonized atlas of mouse spinal cord cell types and their spatial organization. *Nature Communications*, 12(1), 5722. <https://doi.org/10.1038/s41467-021-25125-1>
- Schmid, R. S., Yokota, Y., & Anton, E. S. (2006). Generation and characterization of brain lipid-binding protein promoter-based transgenic mouse

- models for the study of radial glia. *Glia*, 53(4), 345–351. <https://doi.org/10.1002/glia.20274>
- Schnitzer, J., Franke, W. W., & Schachner, M. (1981). Immunocytochemical demonstration of vimentin in astrocytes and ependymal cells of developing and adult mouse nervous system. *The Journal of Cell Biology*, 90(2), 435–447. <https://doi.org/10.1083/jcb.90.2.435>
- Sharifi, K., Ebrahimi, M., Kagawa, Y., Islam, A., Tuerxun, T., Yasumoto, Y., Hara, T., Yamamoto, Y., Miyazaki, H., Tokuda, N., Yoshikawa, T., & Owada, Y. (2013). Differential expression and regulatory roles of FABP5 and FABP7 in oligodendrocyte lineage cells. *Cell and Tissue Research*, 354(3), 683–695. <https://doi.org/10.1007/s00441-013-1730-7>
- Sharifi, K., Morihiro, Y., Maekawa, M., Yasumoto, Y., Hoshi, H., Adachi, Y., Sawada, T., Tokuda, N., Kondo, H., Yoshikawa, T., Suzuki, M., & Owada, Y. (2011). FABP7 expression in normal and stab-injured brain cortex and its role in astrocyte proliferation. *Histochemistry and Cell Biology*, 136(5), 501–513. <https://doi.org/10.1007/s00418-011-0865-4>
- Sharma, K., Schmitt, S., Bergner, C. G., Tyanova, S., Kannaiyan, N., Manrique-Hoyos, N., Kongi, K., Cantuti, L., Hanisch, U. K., Philips, M. A., Rossner, M. J., Mann, M., & Simons, M. (2015). Cell type- and brain region-resolved mouse brain proteome. *Nature Neuroscience*, 18(12), 1819–1831. <https://doi.org/10.1038/nn.4160>
- Snider, K. H., Dziema, H., Aten, S., Loeser, J., Norona, F. E., Hoyt, K., & Obrietan, K. (2016). Modulation of learning and memory by the targeted deletion of the circadian clock gene *Bmal1* in forebrain circuits. *Behavioural Brain Research*, 308, 222–235. <https://doi.org/10.1016/j.bbr.2016.04.027>
- Snider, K. H., Sullivan, K. A., & Obrietan, K. (2018). Circadian regulation of hippocampal-dependent memory: Circuits, synapses, and molecular mechanisms. *Neural Plasticity*, 2018, 7292540. <https://doi.org/10.1155/2018/7292540>
- Storch, K. F., Paz, C., Signorovitch, J., Raviola, E., Pawlyk, B., Li, T., & Weitz, C. J. (2007). Intrinsic circadian clock of the mammalian retina: Importance for retinal processing of visual information. *Cell*, 130(4), 730–741. <https://doi.org/10.1016/j.cell.2007.06.045>
- Takahashi, J. S. (2017). Transcriptional architecture of the mammalian circadian clock. *Nature Reviews. Genetics*, 18(3), 164–179. <https://doi.org/10.1038/nrg.2016.150>
- Tonon, M. C., Desy, L., Nicolas, P., Vaudry, H., & Pelletier, G. (1990). Immunocytochemical localization of the endogenous benzodiazepine ligand octadecaneuropeptide (ODN) in the rat brain. *Neuropeptides*, 15(1), 17–24. [https://doi.org/10.1016/0143-4179\(90\)90155-r](https://doi.org/10.1016/0143-4179(90)90155-r)
- Tonon, M. C., Vaudry, H., Chuquet, J., Guillebaud, F., Fan, J., Masmoudi-Kouki, O., Vaudry, D., Lanfray, D., Morin, F., Prevot, V., Papadopoulos, V., Troadec, J. D., & Leprince, J. (2020). Endozepines and their receptors: Structure, functions and pathophysiological significance. *Pharmacology & Therapeutics*, 208, 107386. <https://doi.org/10.1016/j.pharmthera.2019.06.008>
- Torres-Platas, S. G., Hercher, C., Davoli, M. A., Maussion, G., Labonte, B., Turecki, G., & Mechawar, N. (2011). Astrocytic hypertrophy in anterior cingulate white matter of depressed suicides. *Neuropsychopharmacology*, 36(13), 2650–2658. <https://doi.org/10.1038/npp.2011.154>
- Tyanova, S., Temu, T., & Cox, J. (2016). The MaxQuant computational platform for mass spectrometry-based shotgun proteomics. *Nature Protocols*, 11(12), 2301–2319. <https://doi.org/10.1038/nprot.2016.136>
- Tyanova, S., Temu, T., Sinitcyn, P., Carlson, A., Hein, M. Y., Geiger, T., Mann, M., & Cox, J. (2016). The Perseus computational platform for comprehensive analysis of (prote)omics data. *Nature Methods*, 13(9), 731–740. <https://doi.org/10.1038/nmeth.3901>
- Wink, M. R., Braganhol, E., Tamajusuku, A. S., Lenz, G., Zerbini, L. F., Libermann, T. A., Sevigny, J., Battastini, A. M., & Robson, S. C. (2006). Nucleoside triphosphate diphosphohydrolase-2 (NTPDase2/CD39L1) is the dominant ectonucleotidase expressed by rat astrocytes. *Neuroscience*, 138(2), 421–432. <https://doi.org/10.1016/j.neuroscience.2005.11.039>
- Zougman, A., Selby, P. J., & Banks, R. E. (2014). Suspension trapping (STrap) sample preparation method for bottom-up proteomics analysis. *Proteomics*, 14(9), 1006–1000. <https://doi.org/10.1002/pmic.201300553>

SUPPORTING INFORMATION

Additional supporting information can be found online in the Supporting Information section at the end of this article.

How to cite this article: Bering, T., Gadgaard, C., Vorum, H., Honoré, B., & Rath, M. F. (2023). Diurnal proteome profile of the mouse cerebral cortex: Conditional deletion of the *Bmal1* circadian clock gene elevates astrocyte protein levels and cell abundance in the neocortex and hippocampus. *Glia*, 71(11), 2623–2641. <https://doi.org/10.1002/glia.24443>